

AD-A062 487

BOLT BERANEK AND NEWMAN INC ARLINGTON VA

F/G 17/1

PREDICTION OF PASSIVE SONAR DETECTION PERFORMANCE IN ENVIRONMENT--ETC(U)

NOV 78 M MOLL

N00014-77-C-0303

UNCLASSIFIED

BBN-3656

NL

1 OF 2

AD A062487



**Bolt Beranek and Newman Inc.**



*J*  
*12*

AD A062487

Report No. 3656

**LEVEL**

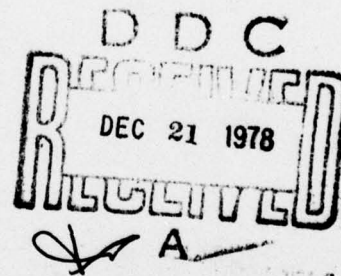
**Prediction of Passive Sonar Detection Performance  
in Environments with Acoustical Fluctuations**

*M. Moll*

DDC FILE COPY

November 1978

Presented to the  
Naval Analysis Programs (Code 431)  
Office of Naval Research



"Reproduction in whole or in part is  
permitted for any purpose of the  
United States Government."

"Approved for Public Release; Distribution Unlimited."

78 12 11 162



Report No. 3656

PREDICTION OF PASSIVE SONAR DETECTION PERFORMANCE IN ENVIRONMENTS WITH  
ACOUSTICAL FLUCTUATIONS

*M. Moll*

November 1978

Contract No. N00014-77-C-0303  
Task No. NR 274-288  
BBN Job No. 10501

Presented to:

Naval Analysis Programs (Code 431)  
Office of Naval Research  
Arlington, VA 22217

Presented by:

Bolt Beranek and Newman Inc.  
1701 North Fort Myer Drive  
Arlington, VA 22209

"Reproduction in whole or in part is  
permitted for any purpose of the  
United States Government."

"Approved for Public Release; Distribution Unlimited."

Unclassified

SECURITY CLASSIFICATION OF THIS PAGE (When Data Entered)

14. REPORT DOCUMENTATION PAGE		READ INSTRUCTIONS BEFORE COMPLETING FORM	
1. REPORT NUMBER BBN-3656	2. GOVT ACCESSION NO.	3. RECIPIENT'S CATALOG NUMBER	
4. TITLE (and Subtitle) Prediction of Passive Sonar Detection Performance in Environments with Acoustical Fluctuations.		5. TYPE OF REPORT & PERIOD COVERED Technical rept.	
7. AUTHOR(S) Magnus/Moll		6. PERFORMING ORG. REPORT NUMBER BBN Report No. 3656	
9. PERFORMING ORGANIZATION NAME AND ADDRESS Bolt Beranek and Newman Inc. 1701 North Fort Myer Drive Arlington, VA 22209		8. CONTRACT OR GRANT NUMBER(S) N00014-77-C-0303	
11. CONTROLLING OFFICE NAME AND ADDRESS Naval Analysis Programs (Code 431) Office of Naval Research Arlington, VA 22217		10. PROGRAM ELEMENT PROJECT TASK AREA & WORK UNIT NUMBERS 6515N NR 274-288 R0145 R0145	
14. MONITORING AGENCY NAME & ADDRESS (if different from Controlling Office) N/A		12. REPORT DATE November 1978	
16. DISTRIBUTION STATEMENT (of this Report) "Approved for Public Release; Distribution Unlimited."		13. NUMBER OF PAGES 123	
17. DISTRIBUTION STATEMENT (of the abstract entered in Block 20, if different from Report) N/A		15. SECURITY CLASS. (of this report) Unclassified	
18. SUPPLEMENTARY NOTES			
19. KEY WORDS (Continue on reverse side if necessary and identify by block number) Passive Sonar Detection Performance Underwater Acoustic Fluctuations			
20. ABSTRACT (Continue on reverse side if necessary and identify by block number) Statistical methods of systems analysis are employed to predict the performance of a passive sonar receiver operating in environments with fluctuating signals and noise. The receiver analog employed is a multichannel processor that produces for each channel a decision threshold that is determined by the outputs of other channels. The receiver inputs are compound random processes exhibiting characteristics observed in experimental studies of ambient noise. The parameters of these processes including their relaxation			

406 454

LB pay

Unclassified

SECURITY CLASSIFICATION OF THIS PAGE (When Data Entered)

20. ABSTRACT (cont'd)

times can be selected to suit a particular set of environmental conditions. The principal objective is to achieve realistic predictions of the probability of detection by single observations. Performance is found to depend on the autocovariance functions of the power envelopes of the fluctuating inputs as well as on their first order probability densities. Transition curves, giving probability of detection as a function of average excess signal-to-noise level, are developed for several cases of fluctuation parameters. Use of these curves for determining the single-look probability of detection merely requires evaluation of the sonar equation to determine the average excess signal-to-noise level for particular sonar operating environments.

ADDITIONAL	
000	White Section <input checked="" type="checkbox"/>
000	Buff Section <input type="checkbox"/>
UNANNOUNCED	<input type="checkbox"/>
JUSTIFICATION	
BY	
DISTRIBUTION/AVAILABILITY CODES	
Dist.	AVAIL. AND SPECIAL
A	

Classified references, distribution  
unlimited-  
No change per Ms. Tomimatsu, ONR/Code  
431

Unclassified

SECURITY CLASSIFICATION OF THIS PAGE (When Data Entered)



Table of Contents

	<u>Page</u>
1.0 PASSIVE SONAR PERFORMANCE ANALYSIS.....	1
2.0 MULTICHANNEL ANALOG.....	11
2.1 Introduction.....	11
2.2 Detection Analysis.....	12
3.0 OUTPUT DENSITY FUNCTION.....	18
4.0 A COMPOUND RANDOM PROCESS.....	26
4.1 Introduction.....	26
4.2 A Class of Compound Processes.....	29
4.3 Power Envelope Processes.....	39
5.0 EVALUATION OF OUTPUT MOMENTS.....	53
6.0 TIME-INVARIANT POWER ENVELOPES.....	74
6.1 Special Case: $P_i(t) = p_N$ .....	74
6.2 Special Case: $P_i(t) = P_N$ .....	78
7.0 SPECIAL CASE: $P_i(t) = P_N(t)$ .....	92
<u>References</u> .....	110
<u>Appendix: An Alternative Approach</u> .....	112
<u>Distribution List</u> .....	117



List of Figures

	<u>Page</u>
FIGURE 1.1 Representation of Multibeam Sonar System.....	3
FIGURE 1.2 Setup for Obtaining Transition Curve.....	6
FIGURE 2.1 A Multichannel Analog for Temporal Processing.....	13
FIGURE 3.1 Probability Density Functions.....	25
FIGURE 4.1 Hour-of-Day Average (over a three-month summer period) Wind Speeds and Underwater Ambient Noise Levels at 315 Hz, as Measured in an Open-ocean, Deep-water Area.....	27
FIGURE 4.2 Probability Density Functions for Amplitude of Random Processes.....	32
FIGURE 4.3 Distribution of Estimates.....	34
FIGURE 4.4 Estimates of Standard Deviation of Noise Ampli- tude for Consecutive Data Sets.....	38
FIGURE 5.1 Plan View of Polygon.....	70
FIGURE 6.1 Transition Curves.....	79
FIGURE 6.2 Probability Error for $a = 1$ , $b = 3$ .....	85
FIGURE 6.3 Probability Error for $a = 1$ , $b = 6$ .....	85
FIGURE 6.4 Probability Error for $a = 3$ , $b = 3$ .....	86

List of Figures (cont'd)

	<u>Page</u>
FIGURE 6.5 Probability Error for $a = 3$ , $b = 6$ .....	86
FIGURE 6.6 Probability Error for $a = 6$ , $b = 3$ .....	87
FIGURE 6.7 Probability Error for $a = 6$ , $b = 6$ .....	87
FIGURE 6.8 Transition Curves for $a = 1$ .....	89
FIGURE 6.9 Transition Curves for $a = 3$ .....	90
FIGURE 6.10 Transition Curves for $a = 6$ .....	91
FIGURE 7.1 Transition Curves for NSC Envelope, $n = 4$ .....	98
FIGURE 7.2 Transition Curves for NSC Envelope, $n = 8$ .....	99
FIGURE 7.3 Transition Curves from Non-normal Basis.....	109

List of Tables

	<u>Page</u>
Table 1. Third Central Moment of Test Statistic.....	63
Table 2. Evaluation of Third Central Moment.....	68



## 1.0 PASSIVE SONAR PERFORMANCE ANALYSIS

By the end of World War II, available methods for predicting and analyzing the detection performance of sonar systems were well documented in the Underwater Sound series of the summary reports produced for the National Defense Research Committee. These methods can be summarized by two entities: the sonar equation and the receiver transition curve.

The objective of this report is to develop methods for predicting the performance of passive sonars operating in environments with fluctuating sonar equation parameters. Although this subject has received considerable attention in the last two decades, nearly all of the effort pertains to cases in which the relaxation time of the fluctuations is large compared to the post-rectification averaging time. The end product of the development is a set of transition curves applicable to a limited set of fluctuating acoustic environments. The use of these curves requires evaluation of this sonar equation to determine the average excess signal-to-noise level for particular sonar operating environments.

The remainder of this section discusses the rationale and utility of the sonar equation and the transition curve, and identifies the essence of the current state-of-the-art. This discussion serves as an introduction for a description of certain salient features of the approach followed in the remainder of the report, and also serves as a framework for the utilization of the resulting receiver transition curves.



A block diagram of a broadband multibeam sonar system is given in Figure 1.1, in which the heavy arrows indicate multiple paths. Only one of numerous sources of background noise is represented. The prediction problem can be divided into two parts, as suggested by the vertical dashed line. To the left of that line, there are components that are generally regarded as having linear transfer characteristics, such as the acoustic transmission channel, the sensor elements of the array, and the bandpass filters of the receivers. The beam-forming operation may be linear or nearly so, or be non-linear when the inputs are hard-clipped. If all of the components are linear, then the concept of signal power and noise power at the outputs of the bandpass filters is unambiguous. The principal difficulty here is predicting the characteristics of the acoustic transmission channel from the source of interest to the array.

A variety of processing functions are performed in the portion of the system on the right side of the dashed line. Each receiver includes a rectifier, a device with an inherently non-linear transfer characteristic. The outputs of the rectifiers are shown on an intensity - or reflectance modulated display in a beam-time format. An operator views the display from time to time and makes decisions regarding the presence of the source of interest. The analysis of operator performance is considered a very difficult undertaking; however, recent researches in neurophysiology\* have produced information regarding important functions performed in the human visual perception system.

---

\*Reviewed in Section 2.0 of Reference 4.

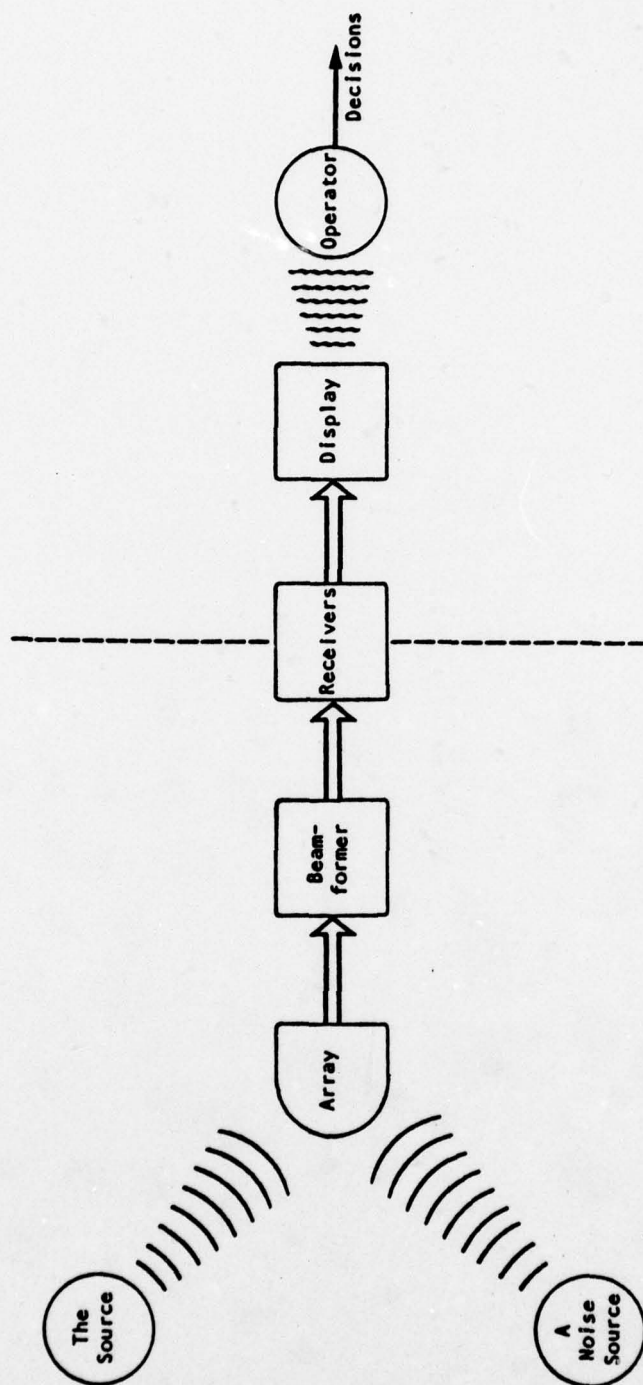


FIGURE 1.1 Representation of Multibeam Sonar System.

Given these complexities, it has been found expedient to consider the elements to the right of the dashed line as a unit, and to characterize their combined performance by means of a transition curve that can be obtained experimentally. A transition curve gives the probability  $P_D$  that the operator will detect the presence of the source of interest with one observation of the display, as a function of the difference  $N_B$  of the average signal level and the average noise level that would be measured at the output of a bandpass filter of the beam directed at the source of interest. The value  $N_D$  of  $N_B$  for which  $P_D$  equals a specified value is called the detection differential, or the recognition differential if classification of the source is achieved. Usually the value specified for  $P_D$  is 0.5. The asymptotic value for  $N_B \rightarrow -\infty$  is  $P_F$ , the probability of false alarm for a single observation. If the operator has an option regarding the duration of record displayed, then the chosen option should be specified.

A transition curve can be plotted as a function of  $N_B$ , or as a function of  $N_E = N_B - N_D$ . The quantity  $N_E$  is usually called the signal excess, although it is defined in terms of signal and noise level differences. If the dependence of  $N_D$  on record duration is known, then one curve will likely suffice for all of the duration options, provided that no other display parameters are changed.

A single transition curve does not completely characterize the combined operation of the components to the right of the dashed line. A different curve could obtain if the power fluctuations of the inputs were distributed differently, or if the time scales of those fluctuations were different, as will be seen in Section 7.0



It is difficult to obtain data for a transition curve under actual operating conditions because of the problem of determining the signal level at the output of the receiver bandpass filter when it is much less than the noise level. Figure 1.2 shows a means for obtaining the curve under laboratory conditions. Signal levels would be varied, and numerous observations would be made by several or more operators. The relevance of the curve to a particular environment will depend on the degree to which the statistics of the inputs approach those under operating conditions.

Given the appropriate transition curve as a function of  $N_E$ , the remaining task is to find the value of  $N_E$  achieved by the sonar system under specified operating conditions. This is usually done by means of the sonar equation

$$N_E = L_S - N_W - L_N + N_A - N_D \quad (1.1)$$

where  $L_S$  is the source level in the receiver passband

$N_W$  is the propagation loss

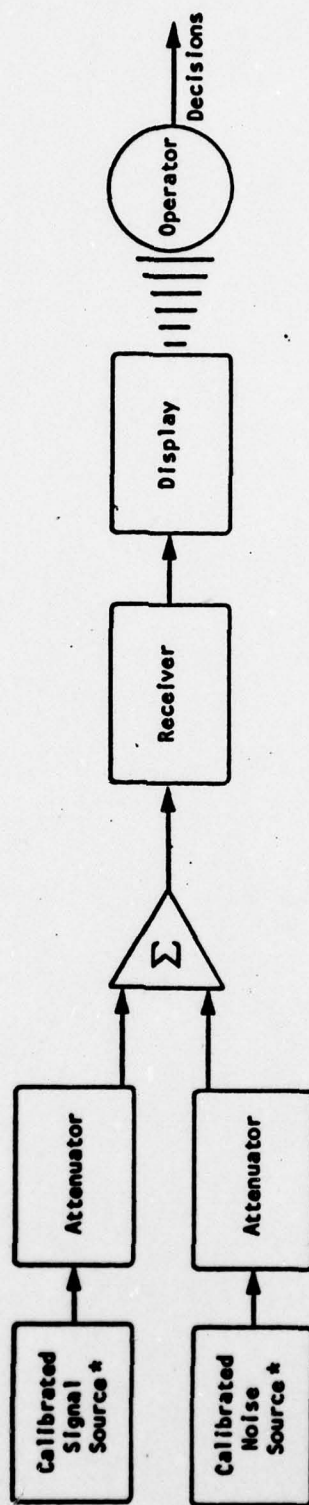
$L_N$  is the noise level at the array in the receiver passband

$$N_A = 10 \log G_S - 10 \log G_N$$

$G_S$  is the average signal power gain of the array over the receiver passband

$G_N$  is the average noise power gain of the array over the receiver passband





\* Either of these might be high-quality field recordings.

FIGURE 1.2 Setup for Obtaining Transition Curve.

If  $N_E$  is identically zero in (1.1), the result is the sonar detection threshold equation; solving that equation for  $N_W$  gives the figure of merit, the value of  $N_W$  for which the probability of detection is that specified for  $N_D$ . Using this particular value of  $N_W$  and the appropriate transmission loss curve gives the detection threshold range.

If the sonar system is operated in different environments, then some of the sonar equation values on the right side of (1.1) are not known *a priori*, and they can be regarded as random variables. In that case, it is clear from (1.1) that  $N_E$  is also a random variable. In that case, the single-look probability of detection is given by

$$P_D = E\{g(N_E)\} = \int_{-\infty}^{\infty} dx g(x) f_E(x) \quad (1.2)$$

where  $E$  is the expectation operator

$g(\ )$  is the function specifying the transission curve

$f_E(\ )$  is the probability density function for  $N_E$

If  $N_E$  is broadly distributed compared to the spread of the transission curve, then

$$P_D \approx \int_0^{\infty} dx f_E(x) \quad (1.3)$$

This is equivalent to assuming that  $g(x)$  is a unit step function  $u(x)$ . If the terms on the right of (1.1) are statistically independent, then the distribution of  $N_E$  is readily determined if the distributions of the terms are known. However, the terms may not be independent; for example,  $N_W$  and  $L_N$  may be dependent to the extent that the noise sources are in the propagation medium.

Transition curves can also be obtained by employing the methods of statistical detection theory. This requires that a circuit analog be developed for the components to the right of the dashed line in Figure 1.1. The classical single-channel analog (II.B, Reference 1) includes a square-law rectifier, an averager, and a threshold detector. A multi-channel analog, described in Section 2.0, is applicable to the analysis of a wider variety of input conditions.

The application of detection theory also requires characterizing the inputs statistically. In Section 6.1, the transition curve is obtained for a case in which the inputs are stationary normal stochastic processes. In Section 6.2, the inputs have the form  $\sqrt{P} G(t)$ , where  $P$  is a non-negative random variable with the dimensions of power, and  $G(t)$  is a stationary normal random process with zero mean and unit variance. This analysis leads to a calculation equivalent to (1.2). Several examples are investigated in which  $P$  is a random variable with a gamma distribution. For these cases, the integral in (1.3) yielded convenient closed forms; the accuracy of this approximation was investigated and found to be good.



A more general class of inputs has the form  $\sqrt{P(t)}G(t)$ , where  $P(t)$ , called a power envelope process, is a non-negative stationary random process with dimensions of power. In Section 4.2, it is shown that the statistical properties of this class agree with the results of careful measurements of ambient noise. Section 4.1 discusses the relevance of stationary processes to cases in which the inputs have cyclical non-stationarities whose periods are very large compared to the post-rectification averaging time. Section 4.3 defines and analyzes two classes of power envelope processes.

Section 7.0 produces transition curves for cases in which the noise inputs have power envelopes that are fully correlated. For performance predictions, these curves would be utilized by employing (1.1) to calculate the value of  $N_E$ . In this case,  $N_D$  is that pertaining to stationary normal inputs; it is calculated from

$$N_D = 10 \log \gamma - 5 \log WT \quad (1.4)$$

where  $N(-\gamma) = P_F$

$N( )$  is the normal probability distribution function for a zero-mean, unit-variance, random variable

$P_F$  is the probability of false alarm with normal noise inputs

$W$  is the noise equivalent bandwidth, defined below (5.17)

$T$  is post-rectification averaging time



At the present time, (1.2) represents the state-of-the-art of dealing with the effects of variability of sonar parameters, although (1.3) is more frequently employed. Either applies if one or more of the parameters is a random variable, or if the relaxation time is long compared to the post-rectification averaging time. The method developed in this report does not assume those conditions, and is capable of showing the dependence of performance on the relaxation time of the power envelopes. Figure 7.3, for example, shows transition curves for different values of  $T \div D$ , where  $D$  is the relaxation time of the noise power envelope.

The remainder of the report develops the relations required for calculating the transition curves for the case of the fluctuating power envelope. Section 3.0 develops a means for approximating the probability density of the averager output based on a polynomial expansion and a basis density function. Section 5.0 derives low-order moments of the averager output; these moments are required for the calculation of the coefficients of the polynomial expansion. An alternative to this approach is discussed in the Appendix.

## 2.0 MULTICHANNEL ANALOG

### 2.1 Introduction

Certain functions performed by sonar systems require simultaneous processing of multiple inputs. One example is the processing of multiple broadband preformed beam signals to be displayed in a beam-time format. Another example is a frequency analyzer utilizing either a bank of fixed filters or more likely a discrete Fourier transform algorithm. Here the output format is bin or filter number (representing a frequency band) versus time. In these examples, the channels are discrete; however, each has a continuous analog in which either a beam is swept in azimuth, or an oscillator is swept in frequency to heterodyne signals into a single fixed pass-band. These continuous versions can be represented in discrete forms with contiguous multiple channels with the appropriate bearing or frequency resolution.

The multichannel analog was initially employed [Ref. 1, Section II] to predict the performance of an operator using a multichannel display. It was applied to the case of a broadband multibeam sonar with a beam-time display format. With this approach, it was possible to predict the effects of acoustic interference produced by nearby ships on sonar detection performance. The limiting case of infinite averaging time has been labeled the bias-limited case [2]. A more compact derivation of the performance of the multichannel analog is given in Ref. 3.

A more detailed analysis of the detection performance of an operator using Lofar [4] was based on certain results of neurophysiological and psychophysical studies of the visual

perception system. One result of that analysis showed that the effective frequency resolution of the operator's receptive\* fields could be larger than that of the Lofar processor, and that detection performance could be poorer than that expected on the basis of the analyzer bandwidth. If the multichannel analog is employed, a first-order correction of this discrepancy can be made by selecting the larger value of bandwidth.

A schematic of the multichannel analog is shown in Figure 2.1. The representation is vectorial in that it represents multiple signal flow and multiple (but similar) components in single blocks. The outputs of the averagers are a set of quantities  $\underline{Y} = \{Y_1\}$ . In the classical circuit analog [Ref. 1, pp. 8-14], each of these would be compared to a fixed threshold to form the basis for a detection decision. In the multichannel analog, however, a quantity  $Z_k$  is formed for each channel that is the difference between the averager output  $Y_k$  and a quantity  $W_k$  that is a linear combination of the averager outputs  $Y_1$ ,  $1 \neq k$ . If the quantity  $Z_k$  is greater than zero, a detection would be declared. This scheme is equivalent to that described in Refs. 1 and 3 in which  $Y_k$  is compared to a threshold  $W_k$ . The advantage of the formulation shown in Figure 2.1 is that the basis for decisions is a single random vector  $\underline{Z}$  instead of the pair  $\underline{Y}$  and  $\underline{W}$ .

## 2.2 Detection Analysis

If the post-rectification averaging is uniform for a time period  $T$ , then the output of the  $i$ th averager can be expressed as

\*The receptive field of a neuron in the visual system is defined as that portion of the retina (or the corresponding visual field) that produces a response in the neuron when stimulated by light.



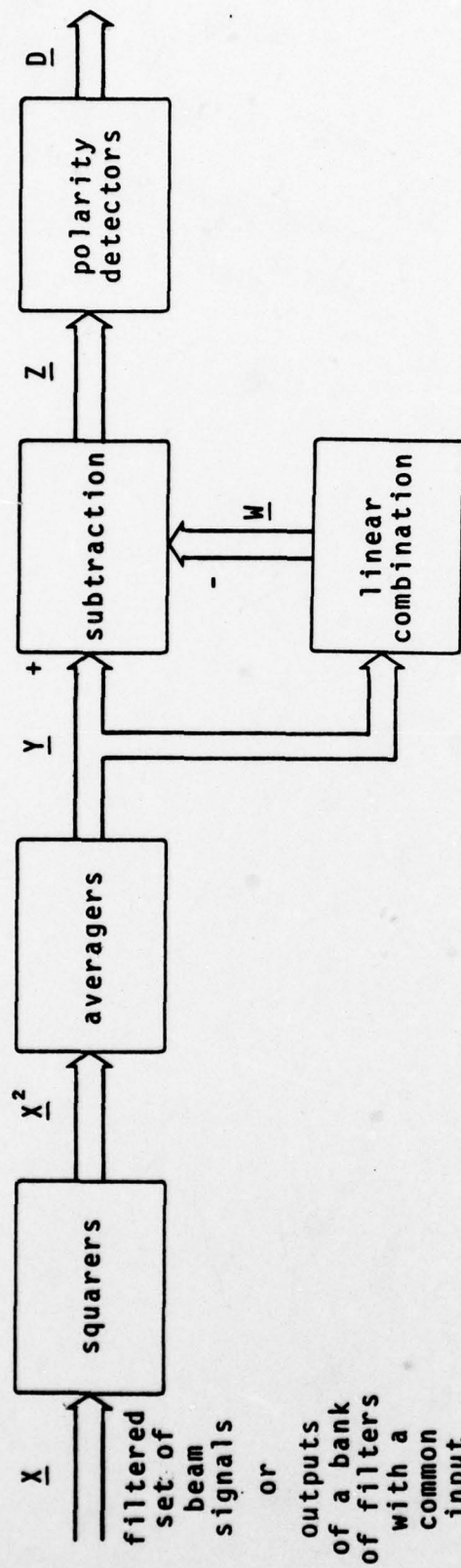


FIGURE 2.1 A Multichannel Analog for Temporal Processing.

$$Y_1(t) = T^{-1} \int_{t-T}^t du X_1^2(u) \quad (2.1)$$

If the inputs are stationary, then the steady-state probability measures are invariant with time, and it will be convenient to evaluate the output at time  $T$ :

$$Y_1 = T^{-1} \int_0^T du X_1^2(u) \quad (2.2)$$

If no signal is present in channel 1, then the output to its squarer is

$$X_1(t) = N_1(t) \quad (2.3)$$

and the output of its averager is

$$Y_1(t) = T^{-1} \int_0^T du N_1^2(u) \quad (2.4)$$

And if a signal is present in channel 0 (zero), then the input to its squarer is

$$X_0(t) = N_0(t) + S(t) \quad (2.5)$$

and the output of its averager is

$$Y_0(t) = T^{-1} \int_0^T du [N_0^2(u) + 2N_0(u)S(u) + S^2(u)] \quad (2.6)$$

where  $S(t)$  is the signal component of the input to channel 0.

Per the discussion in Section 2.1, the test statistic for channel 0 is

$$Z = Y - W \quad (2.7)$$

$$= Y - \sum_{i=1}^n c_i Y_i \quad (2.8)$$

where  $c_i$  is the weighting coefficient for channel  $i$ . To simplify the notation, the subscript zero will be suppressed except to designate the noise component of the input to that channel. Substituting (2.4) and (2.6) in (2.8) gives

$$Z = T^{-1} \int_0^T du [S^2(u) + 2S(u)N_0(u) - \sum_{i=0}^n c_i N_i^2(u)] \quad (2.9)$$

where the noise term for the channel of interest is included in the summation by setting  $c_0 = -1$ .

The probability that the test statistic  $Z$  exceeds the (zero) threshold is

$$P(Z \geq 0) = \int_0^{\infty} dz f_Z(z) \quad (2.10)$$

where  $f_Z(\ )$  is the probability density function for the test statistic  $Z$ . It will be convenient to consider the standardized random variable

$$Q = \frac{Z - m_Z}{\sigma_Z} \quad (2.11)$$



where  $m_Z$  and  $\sigma_Z$  are the mean value and standard deviation of  $Z$  respectively. Then the probability that the test statistic  $Z$  exceeds the threshold is

$$\begin{aligned} P(Z \geq 0) &= P(Q \geq -m_Z / \sigma_Z) \\ &= \int_{-m_Z / \sigma_Z}^{\infty} dq f_Q(q) \end{aligned} \quad (2.12)$$

where  $f_Q(q) = f_Z(\sigma_Z q + m_Z)$  is the probability density function for the standardized random variable  $Q$ . The (conditional) probability of detection is then

$$\begin{aligned} P_D &= P(Z \geq 0 | p_S > 0) \\ &= \int_{-m_{ZS} / \sigma_{ZS}}^{\infty} dq f_Q(q | p_S > 0) \end{aligned} \quad (2.13)$$

where  $p_S$  is the mean square value of  $S(t)$

$$m_{ZS} = E(Z | p_S > 0)$$

$$\sigma_{ZS} = \sigma(Z | p_S > 0)$$

And the probability of false alarm is

$$\begin{aligned} P_F &= P(Z \geq 0 | p_S = 0) \\ &= \int_{-m_{ZN} + \sigma_{ZN}}^{\infty} dq f_Q(q | p_S = 0) \end{aligned} \quad (2.14)$$

where  $M_{ZN} = E(Z | p_S = 0)$

$$\sigma_{ZN} = \sigma(Z | p_S = 0)$$

The bases for further analysis are (2.13) for the probability of detection on a single observation, (2.14) for the probability of false alarm on a single observation, (2.11) for the standardized random variable, and (2.9) for the test statistic.

### 3.0 OUTPUT DENSITY FUNCTION

As shown in the previous section, the calculation of the probabilities of detection and false alarm requires the probability distribution of the standardized form of the test statistic. The latter is a linear combination of the outputs of integrators with non-Gaussian inputs. The general problem of determining the required distribution function is difficult. Papoulis (Ref. 5, p. 324) states:

"The determination of the distribution  $F_S(s)$  of  $S$  [integrator output] is, in general, hopelessly complicated. After all,  $S$  is the limit of a sum of [random variables], and as we know, even to find the distribution of the sum of only two random variables is not a trivial matter. For this reason we shall not be concerned with  $F_S(s)$ , but shall determine only the mean and variance of  $S$ ."

The same remark applies as well to the probability density function of  $S$ .

Cramer has shown (Ref. 6, Ch. 12, Sec. 6) that a probability density function can be determined from its moments. A density function  $g(x)$  can be expanded in the form

$$g(x) = f(x) \sum_{i=0}^{\infty} b_i p_i(x) \quad (3.1)$$

where  $f(x)$  is a selected density function

$b_i$  are constants to be determined

$p_i(x)$  is an  $i$ th-order polynomial satisfying the condition



$$\int_{-\infty}^{\infty} dx f(x) p_m(x) p_n(x) = \begin{cases} 1 & \text{for } m = n \\ 0 & \text{for } m \neq n \end{cases} \quad (3.2)$$

The coefficients of the polynomial are determined by the moments of  $f(x)$ , and the coefficients explicit in (3.1) are given by

$$b_n = \int_{-\infty}^{\infty} dx p_n(x) g(x) \quad (3.3)$$

Since  $p_n(x)$  is a polynomial in  $x$ , it is seen that  $b_n$  is determined jointly by the coefficients of the polynomial and the moments of  $g(x)$ .

An approximation of  $g(x)$  is obtained by using a finite number of terms in the expansion. One expects that the approximation will be good if  $f(x)$  is itself a reasonably good approximation to  $g(x)$ . If the series (3.1) is terminated at a finite number of terms, then the coefficients of like powers of  $x$  can be summed to obtain an expansion of the form

$$h(x) = f(x)P(x) \quad (3.4)$$

where  $P(x) = \sum_{i=0}^n a_i x^i$

Since  $h(x)$  is to approximate a probability density function, it appears reasonable to require that

$$\int_{-\infty}^{\infty} h(x) x^k dx = \alpha_k, \quad k = 0, 1, 2, \dots, n \quad (3.5)$$

where  $\alpha_k$  is the  $k$ th moment of  $g(x)$ . Equations (3.5) require that  $\int_{-\infty}^{\infty} dx h(x) = 1$ , one requisite of any probability density function, and that the first  $n$  moments of  $h(x)$  equal those of  $g(x)$ . Substituting (3.4) in (3.5) and evaluating the integrals gives

$$\sum_{i=0}^n a_i m_{k+1} = \alpha_k, \quad k = 0, 1, 2, \dots, n \quad (3.6)$$

where  $m_j$  is the  $j$ th moment of the basis function  $f(x)$ , and  $\alpha_0 = 1$ .

In Section 2.0, the probability of detection is expressed as an integral of the probability density function of a standardized random variable; for such a variable, the mean is zero, the variance one, and all moments are central. If both  $g(x)$  and the basis function  $f(x)$  are densities for standardized random variables, then the matrix and vector representing (3.6) for  $n = 3$  are as shown below:

$$\begin{array}{ccccc} 1 & 0 & 1 & m_3 & 1 \\ 0 & 1 & m_3 & m_4 & 0 \\ 1 & m_3 & m_4 & m_5 & 1 \\ m_3 & m_4 & m_5 & m_6 & \alpha_3 \end{array} \quad (3.7)$$

It is easy to show that the coefficients  $a_1$ ,  $a_2$ , and  $a_3$  are proportional to the difference of the third moments  $\alpha_3 - m_3$ . For example, to solve for  $a_2$  by Cramer's rule, replace the third column of the matrix by the vector, and then subtract the elements of the

first column from the new third column. The result is a column with all zeros except for the fourth element  $\alpha_3 - m_3$ . If the determinant is expanded in terms of the elements of this column and their minors, it is apparent that  $a_2$  is proportional to the difference of third moments  $\alpha_3 - m_3$ . A similar procedure applies to  $a_1$  and  $a_3$ .

The method is attractive in that it requires relatively few moments of the test statistic. Its mean and variance are required for (2.13) and (2.14) for the probabilities of detection and false alarm. For the case just discussed, the third moment is also required. Although the mean value is easily obtained, the derivation of the variance and higher moments requires considerable effort. For the basis function  $f(x)$ , on the other hand, the number of moments required is twice that for  $g(x)$ . However, the problem of obtaining these moments is usually not difficult. For many density functions, the characteristic function is available for generating the moments, or in some cases, formulas for the moments are given, as in Reference 7. In any case, (3.5) can be applied with  $h(x)$  replaced by  $f(x)$ , and  $\alpha_k$  by  $m_k$ .

For  $n = 3$ , the polynomial may be expressed as

$$P(x) = 1 + (\alpha_3 - m_3) A^{-1} \sum_{i=0}^3 \delta_i x^i \quad (3.8)$$

where  $A = \delta + \delta_0 m_3$



$$\delta = \begin{vmatrix} m_4 - m_3^2 - 1 & m_5 - m_3(m_4 + 1) \\ m_5 - m_3m_4 & m_6 - m_4^2 \end{vmatrix}$$

$$\delta_0 = \begin{vmatrix} 1 & m_3 \\ m_4 - m_3^2 & m_5 - m_3m_4 \end{vmatrix}$$

$$\delta_1 = \begin{vmatrix} m_3 & m_4 \\ m_4 - 1 & m_5 - m_3 \end{vmatrix}$$

$$\delta_2 = \begin{vmatrix} m_3 & m_5 - m_3 \\ 1 & m_4 \end{vmatrix}$$

$$\delta_3 = \begin{vmatrix} 1 & m_3 \\ m_3 & m_4 - 1 \end{vmatrix}$$

In many cases of interest  $g(x)$  will be approximately normal, and the normal density function is an appropriate basis for the expansion. For this case, all odd-order moments of  $f(x)$  are zero,  $m_4 = 3$ , and  $m_6 = 15$ . Evaluating (3.8) and substituting the result in (3.4) gives

$$h(x) = n(x) [1 - \alpha_3(x/2 - x^3/6)] \quad (3.9)$$

where  $n(x)$  is the density for a normal variate with zero mean and unit variance. The coefficients  $a_1$  through  $a_3$  are seen to be proportional to  $(\alpha_3 - m_3)$ , since  $m_3 = 0$  for this basis function.

In view of the relationship between the Hermite polynomials and the derivatives of  $n(x)$ , it can be shown that an alternative form for (3.9) is [Ref. 6, pp. 222-223]

$$h(x) = n(x) - \frac{\alpha}{6} n^{(3)}(x) \quad (3.10)$$

Substituting this result in (2.12) and evaluating the integrals gives

$$P(Z \geq 0) = N\left(\frac{m_Z}{\sigma_Z}\right) + \frac{1}{6} \cdot \frac{\mu_{3Z}}{\sigma_Z^3} n^{(2)}\left(\frac{m_Z}{\sigma_Z}\right) \quad (3.11)$$

where  $N(\ )$  is the probability distribution function for a normal random variate with zero mean and unit variance.

This is a very convenient form since tables of both  $N(\ )$  and  $n^{(1)}(\ )$  are available.

In Section 2.0, the output of the multichannel analog (2.7) was expressed as

$$Z = Y - W \quad (3.12)$$

where  $Y$  is the output of the averager of the channel of interest

$W$  is a threshold function synthesized from the averager outputs of other channels.

The former ( $Y$ ) is non-negative, and the latter ( $W$ ) will also be if none of the weighting coefficients  $a_i$  in (2.8) are negative. Given these conditions, the probability density of  $Z$  can be expressed as

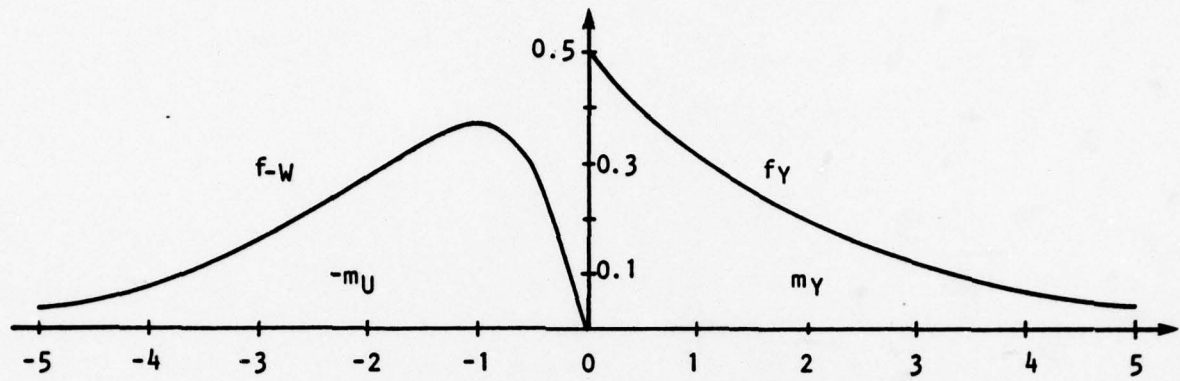
$$f_Z(z) = \int_0^{\infty} dx f_{YW}(x + z, x), \quad z \geq 0 \quad (3.13)$$

$$= \int_0^{\infty} dx f_{YW}(x, x - z), \quad z < 0 \quad (3.14)$$

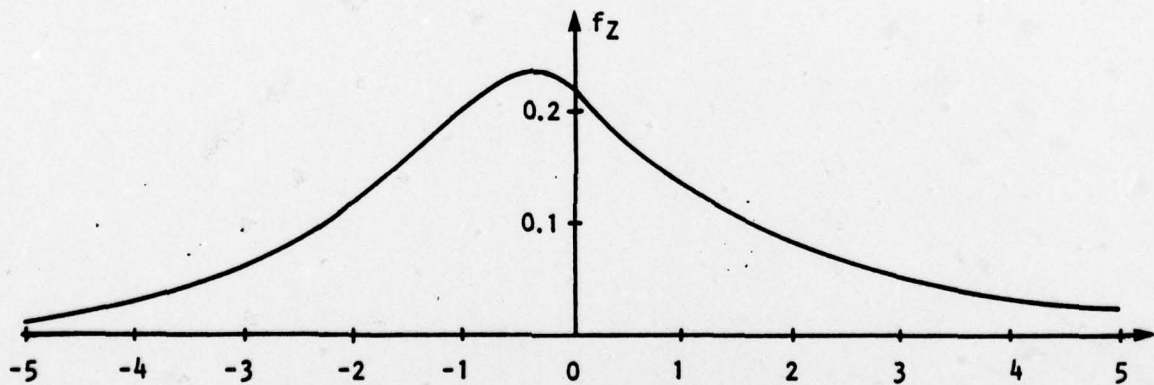
where  $f_{YW}(\cdot)$  is the joint density function for Y and W. Unless Y and W are completely dependent, the variate Z will be bipolar; furthermore, the density function is continuous at  $z = 0$  as can be seen from (3.13) and (3.14).

To illustrate how the density function of the test statistic Z compares to that of the averager output Y of the channel of interest, the following extreme case is considered. The averager output Y is chi-square with two degrees of freedom, and the threshold function W is one-half of a chi-square variate with four degrees of freedom, the result of averaging the outputs of the averagers of two adjacent channels. These processes, assumed independent, would result with an extremely small time-bandwidth product. Applying (3.13) and (3.14) to this case yields the density function plotted in the lower part of Figure 3.1. The function is continuous everywhere, as is its first derivative. The upper part of Fig. 3.1 shows the density functions for Y and -W. The former is discontinuous at zero, as is the first derivative of the latter. The result of the combination via (3.12) yields a test statistic that is more nearly normal than the output of the averager of the channel of interest. For the example selected coefficients of skewness and kurtosis are 0.82 and 6 respectively for the former, and 1 and 9 respectively for the latter.





$x$ , distribution parameter of  $Y$  and  $-W$ .



$z$ , distribution parameter of  $Z$ .

FIGURE 3.1 Probability Density Functions.

#### 4.0 A COMPOUND RANDOM PROCESS

##### 4.1 Introduction

The results of several experimental studies (Refs. 8 and 9) of ambient noise may be summarized as follows:

1. Estimates of first-order probability measures obtained from relatively short segments (compared to certain relaxation times of the process) of sample functions supported, more often than not, the hypothesis that the amplitude of noise in a specified bandpass is distributed normally.
2. The number of departures from first-order normality increased with sample length (Ref. 8, Tables V and VI.)
3. Estimates exhibited more variability than consistent with a stationary Gaussian process.

The first-order probability measures include the distribution function and several of its low-order moments.

It will be shown in the next section that similar results could be expected by observing a stationary compound random process that is conditionally non-stationary normal.

A complete process model for ambient noise would be non-stationary because of dependence on phenomena with cycles such as diurnal, lunar, or annual. Figure 4.1 shows, for example,

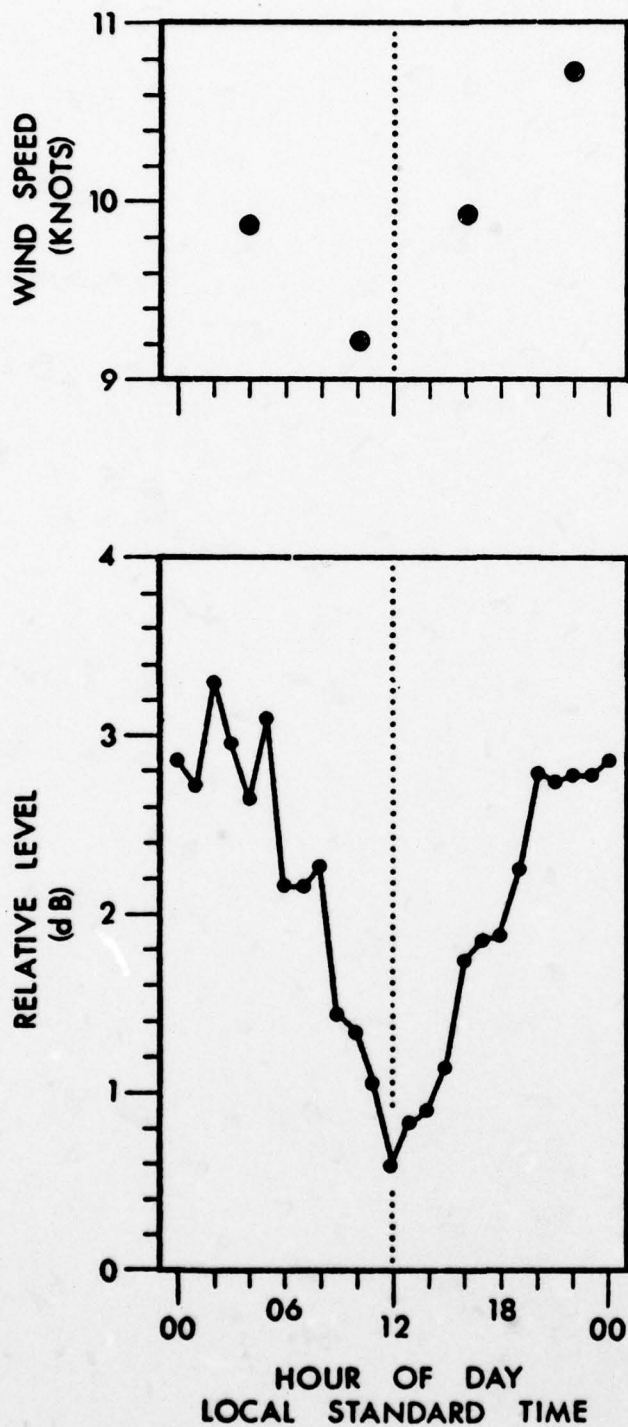


FIGURE 4.1 Hour-of-day Average (over a three-month summer period) Wind Speeds and Underwater Ambient Noise Levels at 315 Hz, as Measured in an Open-ocean, Deep-water Area.  
Source: G.M. Wentz, "Review of Underwater Acoustic Research: Noise."  
JASA Vol. 51, No. 3 (Part 2), March 1972.



the dependence of noise power level on time of day. There may also be long-term trends due to evolution of the generating phenomena, for example, the active ship population.

If, however, the variation of process parameters is small during a period of interest, the process may be considered as locally stationary during that period, and approximated by a stationary process with parameters that are appropriate to the time. If the shortest cycle is diurnal, and if the post-rectification averaging period does not exceed an hour, this approach should be entirely satisfactory for the objectives of this investigation.

A further requirement for the model is that its mean value be zero. This requirement would be met by any stationary process that is the output of either a high-pass or band-pass network or operation. For example, the  $r$ th complex coefficient of the discrete Fourier transform is

$$A_r = \sum_{k=0}^{n-1} X_k \exp(-j2\pi rkn^{-1}) \quad (4.1)$$

where  $X_k$  is the  $k$ th sample of the input (assumed stationary) in the frame. The expected value of the coefficient is

$$E(A_r) = m_X \sum_{k=0}^{n-1} \exp(-j2\pi rkn^{-1}) \quad (4.2)$$

where  $m_X = E(X_k)$ , all  $k$ . It is easily seen from (4.2) that for  $r = mn$ ,  $n = 0, 1, 2, 3, \dots$ , that the value of the indicated sum is  $n$ . This set of outputs represents the low-pass output

and its aliases. For other values of the index  $r$ , the geometric progression defined by the sum is

$$\Sigma = \frac{1 - \exp(-j2\pi r)}{1 - \exp(-j2\pi r n^{-1})} \quad (4.3)$$

The numerator is zero for all  $r$ , and the denominator is not except for  $r = mn$ . Thus

$$\begin{aligned} E(A_r) &= nm_X, \quad r = mn, \quad n = 0, 1, 2, 3, \dots \\ &= 0, \quad r \text{ an integer} \neq mn \end{aligned} \quad (4.4)$$

This set of outputs represents a set of bandpass outputs and their aliases. This result has been demonstrated experimentally (Ref. 9, Page 68).

#### 4.2 A Class of Compound Processes

A fairly broad class of random processes exhibiting the behavior described in the previous section is the compound process

$$N(t) = \sqrt{P(t)} G(t) \quad (4.5)$$

where  $P(t)$  is a non-negative stationary random process.

$G(t)$  is a zero-mean, unit-variance, Gaussian process, statistically independent of  $P(t)$ .

The class, briefly described in Pages 153-154 of Ref. 10, is broad in that the only constraint on  $P(t)$  is that it not be

negative. It is clear from (4.5) that given  $P(t)$ , the process  $N(t)$  is conditionally non-stationary Gaussian.

The compound process defined by (4.5) includes two sub-cases of more than passing interest. In one of these, the power envelope  $P(t)$  is a random variable  $P$  independent of time; in this case, the compound process is non-ergodic, since time averages of individual members would generally not be equal to ensemble averages. Since  $\sqrt{P}$  is not negative, the compound process  $\sqrt{P}G(t)$  is a special case of a spherically invariant process  $A G(t)$ , in which  $A$  is a random variable that is not necessarily non-negative (Ref. 11). In the second case, the power envelope is a deterministic constant, and the compound process degenerates to a Gaussian process (ergodic, and non-compound). Both of these special cases will be considered further in Section 6.0.

The probability density function for  $N(t)$  can be expressed as

$$f_N(n) = \sqrt{2/\pi} \int_0^{\infty} dx f_P(x^2) \exp \left[ -\frac{1}{2} (n/x)^2 \right] \quad (4.6)$$

where  $f_P(\ )$  is the probability density function for  $P(t)$ . It is clear from (4.6) that the function has even symmetry around  $n = 0$ ; hence, all odd-order moments about zero are zero including the first, which satisfies one of the requirements stated in the previous section. Furthermore, all even-order moments are moments about the mean.

For purposes of illustration, consider a case in which  $P(t)$  is a chi-square variable with four degrees of freedom. Application of (4.6) to this case yields



$$f_N(n) = \frac{1}{4} (1 + |n|) \exp(-|n|) \quad (4.7)$$

which is plotted in Figure 4.2 along with the density for a normal variate with the same variance. The departure from normality is quite evident from the density functions; the departure would be less evident from the corresponding distribution functions.

Even-order moments are readily calculated from the corresponding powers of (4.5), the square of which is

$$N^2(t) = P(t)G^2(t) \quad (4.8)$$

If the relaxation time of  $P(t)$  is very large compared with that of the normal process  $G(t)$ , then it seems reasonable to regard the former as a power envelope process. The second moment of the compound process is

$$\sigma_N^2 = E[N^2(t)] = E[P(t)] E[G^2(t)] = p \quad (4.9)$$

where  $p = E[P(t)]$

The fourth central moment of  $N(t)$  is

$$\begin{aligned} \mu_4 &= E[G^4(t)] E[P^2(t)] \\ &= 3(p^2 + \sigma^2) \end{aligned} \quad (4.10)$$

where  $\sigma^2$  is the variance of  $P(t)$ .

solid curve: compound process  
dashed curve: normal process

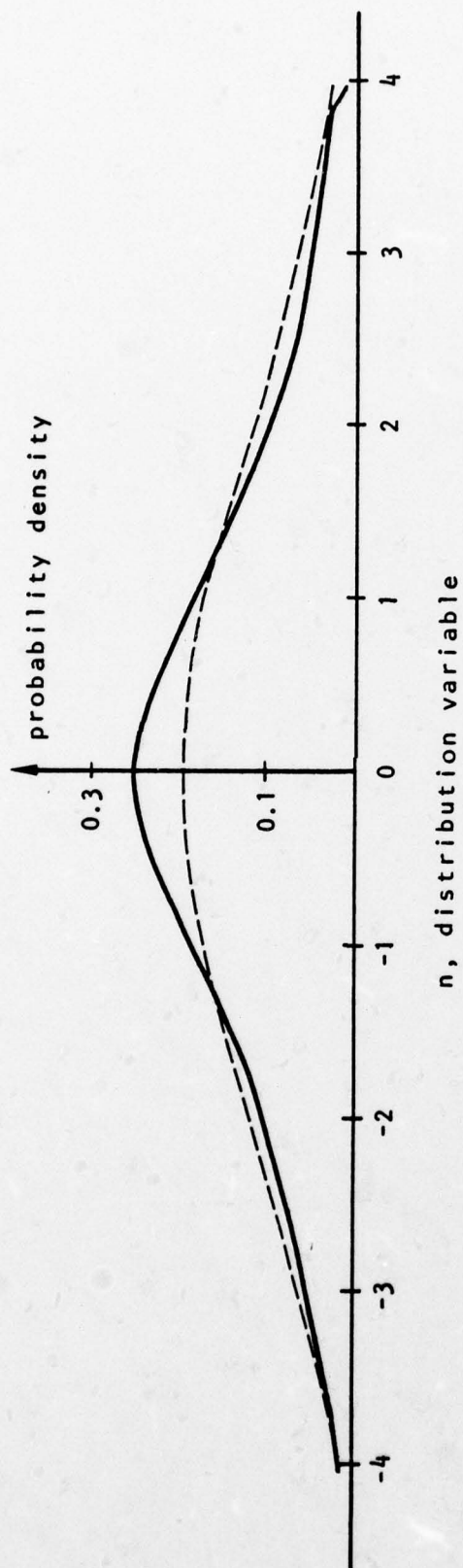


FIGURE 4.2 Probability Density Functions for Amplitude of Random Processes.

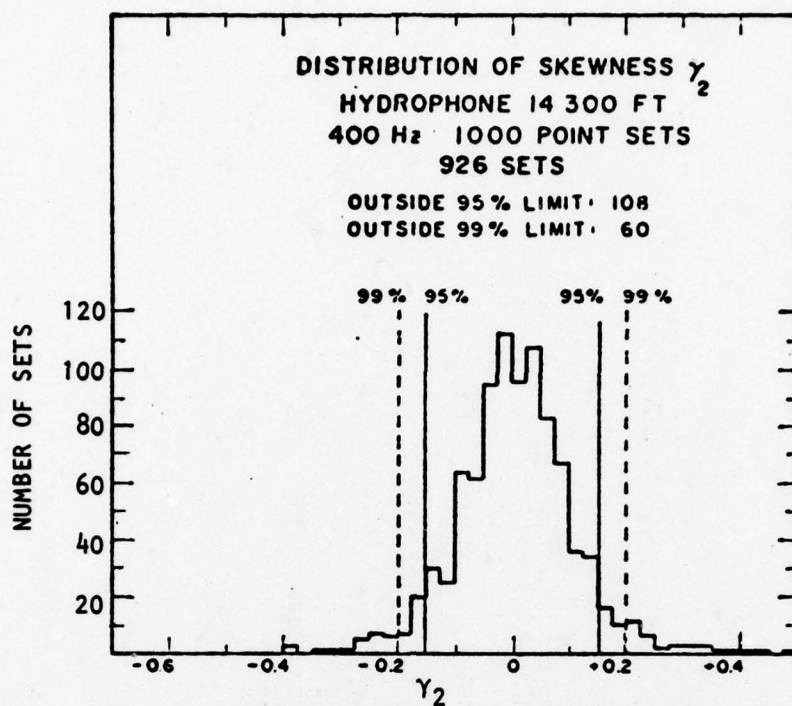
The departure from first-order normality of the compound process can be gauged by comparing its moments to those of corresponding order of a normal variate. For a zero-mean normal variate, all odd-order moments are zero, as is the case for the compound process given by (4.5); thus, for both of these processes the coefficient of skewness  $\mu_3 \div \sigma^3$  is zero. Figure 4.3(a) shows the distribution of sample estimates of that coefficient obtained by Arase and Arase for deep-sea ambient noise. The distribution is fairly even about zero, and about 12 percent of the sample values fall outside of the 95 percent confidence limits. For a normal variate, only 5 percent of the values are expected outside these limits.

The kurtosis of a distribution is defined as  $\mu_4 \div \sigma^4$ . Figure 4.3(b) shows the distribution of kurtosis estimates for deep-sea ambient noise obtained by Arase and Arase. In this case about 28 percent of the values are outside the 95 percent confidence limits, whereas only 5 percent would be expected for a normal variate. Utilization of (4.9) and (4.10) shows that the kurtosis for the compound random process is

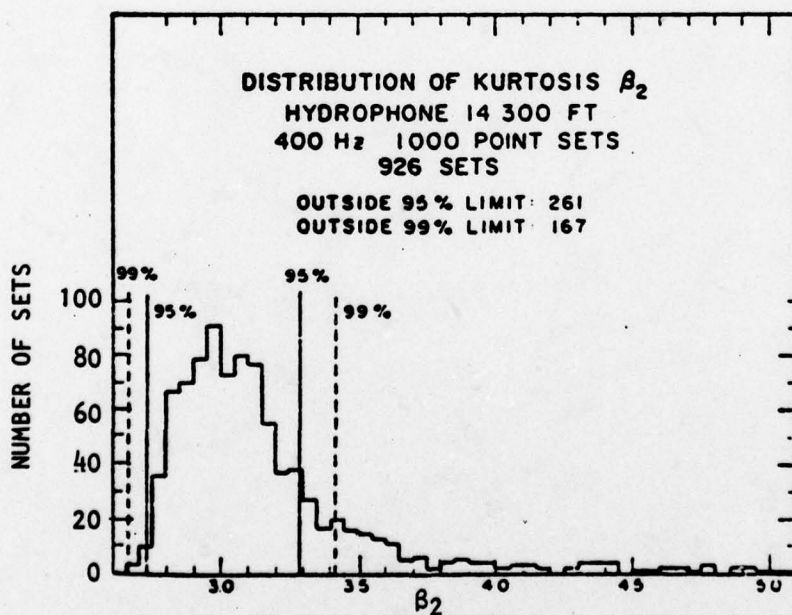
$$\mu_4 \div \sigma_N^4 = 3 [1 + (\sigma/p)^2] \quad (4.11)$$

Thus, if the variance of the power envelope process is greater than zero, the kurtosis of the compound process is greater than three, the kurtosis of a normal population. For the compound process whose probability density function is given by (4.7), the value of kurtosis is (4.5). The kurtosis estimates discussed above were obtained from data periods of 10, 20, and 40 seconds, and the normal hypothesis was rejected more often with the longer data periods. It seems reasonable to expect that larger estimates would be obtained with longer sample periods. These





(a) Distribution of skewness.



(b) Distribution of kurtosis.

FIGURE 4.3 Distribution of Estimates.

Source: T. Arase and E.M.Arased, "Deep-Sea Ambient Noise Statistics". JASA Vol. 44, No. 6, 1968, p1683.

experiments were conducted with single hydrophones; beam noise data might be expected to exhibit greater variability because of the highly uneven weighting of responses to the noise sources, which has the effect of reducing the size of the noise source population.

Certain of the temporal characteristics of the compound random process are revealed by low-order moment functions, easily derivable from (4.5). The autocovariance function for the process is

$$\begin{aligned} K_N(u-v) &= E[N(u)N(v)] \\ &= E[\sqrt{P(u)P(v)}] \rho(u-v) \end{aligned} \quad (4.12)$$

where  $\rho(\ )$  is the autocovariance coefficient function for the normal process  $G(t)$ . If the relaxation time of the P-process is much longer than that of the G-process, then

$$K_N(u-v) \approx E[P(u)] \rho(u-v) = pp(u-v); \quad (4.13)$$

that is, the G-process essentially determines the relaxation time of the compound process and thereby its bandwidth. It is usually this bandwidth that serves as the basis for decisions regarding sample intervals and data periods for experimental efforts. The data periods based on this bandwidth may not be very long compared to the longer relaxation times, in which case the number of statistically independent samples will not be adequate to obtain good parameter estimates.

Since the receiver analog includes squarers, the properties of  $Q(t) = N^2(t)$  are important; the second moment function for the square of  $N(t)$  is

$$\begin{aligned} M_Q(u-v) &= E[N^2(u)N^2(v)] \\ &= E[P(u)P(v)] E[G^2(u)G^2(v)] \end{aligned} \quad (4.14)$$

This moment function is seen to involve a fourth-order moment function for  $N(t)$ ; however, the form is degenerate in that there is only one time difference,  $u-v$ . The second factor of (4.14) is a fourth-order moment function (degenerate) for a normal process. This function can be expressed in terms of lower-order properties by using (7.28) of Ref. 12:

$$M_Q(u-v) = [p^2 + K(u-v)] [1 + 2\rho^2(u-v)] \quad (4.15)$$

where  $K(u-v)$  is the autocovariance function for the power envelope process. Given (4.15) and (4.9), it follows that the autocovariance function for the square of the compound process is

$$K_Q(u-v) = K(u-v) + 2[p^2 + K(u-v)]\rho^2(u-v) \quad (4.16)$$

Given the stipulation on relaxation times,

$$K_Q(u-v) \approx K(u-v) + 2(p^2 + \sigma^2)\rho^2(u-v) \quad (4.17)$$

Given that the variance  $\sigma^2$  of the power envelope process is not negligible compared to  $p^2$ , then the relaxation time of the square of the compound process is essentially determined by that of the power envelope process. This is just the reverse of the situation pertaining to the first power of the process, and the



ramifications with regard to the effectiveness of post-rectification smoothing for either detection or power estimation are considerable.

Figure 4.4 shows a time record of the square root of successive estimates of the mean squared amplitude. There is an overall trend in data correlated with a reduction of local wind speed. Within this period about three cycles of shorter periods are evident. (These periods are much longer than the data averaging period, in this case 20 seconds.) Similar behavior would be exhibited by samples from a compound process with a power envelope process exhibiting two relaxation times, the longer of which is related to the relaxation time of wind speed.

All of the data cited lend support to the consideration of (4.5) as a reasonable model for ocean ambient noise.

Analysis of the performance of the multichannel analog requires specification of a vector random process, that is, of a set of random processes. The set is described by

$$N_i(t) = \sqrt{P_i(t)} G_i(t), \quad i = 1, 2, 3, \dots, n \quad (4.18)$$

where  $P_i(t)$  is a non-negative stationary random process with average value  $p_i$ .

$G_i(t)$  is a zero-mean, unit-variance, Gaussian process, statistically independent of  $P_i(t)$ , all  $i$ , and statistically independent of  $G_j(t)$ , all  $j$  except  $i$ .

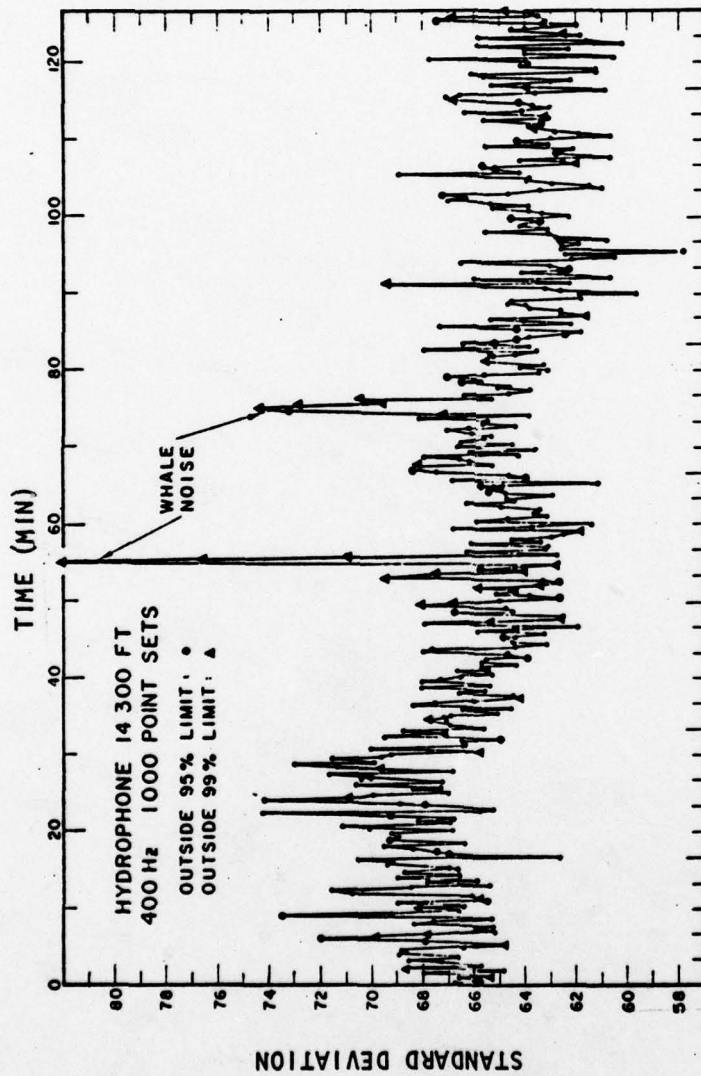


FIGURE 4.4 Estimates of Standard Deviation of Noise Amplitude for Consecutive Data Sets.

Source: T. Arase and E. M. Arase, "Deep-Sea Ambient Noise Statistics" JASA Vol 44, No. 6, 1968, pp 1679-1684.

The assumed mutual independence of the Gaussian processes would be approximated by beamformer outputs in a band of frequencies near the design frequency of the array. Note that the power envelope processes  $P_1(t)$  may be mutually dependent.

The mean value of the  $i$ th member is

$$E[N_1(t)] = 0 \quad (4.19)$$

and the cross-covariance is

$$\begin{aligned} K_{1j}(u-v) &= p_1 \rho_1(u-v), \quad j = 1 \\ &= 0, \quad j \neq 1 \end{aligned} \quad (4.20)$$

The square of the  $i$ th process is

$$N_1^2(t) = P_1(t) G_1^2(t) \quad (4.21)$$

and its average value is

$$E[N_1^2(t)] = p_1 \quad (4.22)$$

Higher order moments are evaluated in Section 5.0.

#### 4.3 Power Envelope Processes

This section introduces power envelope processes that can be employed in the class of compound random processes discussed in Section 4.2. Statistical properties including lower-order moment functions are derived.



The first power envelope process, which may be termed a normalized chi-square process, is an obvious extension of the chi-square random variable:

$$P(t) = pn^{-1} \sum_{i=1}^n G_i^2(t) \quad (4.23)$$

where  $p > 0$  is a constant with dimensions of power;  $G_1(t)$  is a stationary Gaussian process with zero mean and unit variance, statistically independent of  $G_j(t)$ ,  $j \neq 1$ . It is clear from (4.23) and the stipulation above that  $P(t) \geq 0$ . Given the properties of the Gaussian processes  $G_i(t)$  stated above, the mean value of  $P(t)$  is

$$m_P = p \quad (4.24)$$

The second moment function of  $P(t)$  is

$$E[P(u)P(v)] = (pn^{-1})^2 \sum_{i=1}^n \sum_{j=1}^n E[G_i^2(u)G_j^2(v)] \quad (4.25)$$

For  $i \neq j$ , the fourth-order moment function in the summand is

$$E[G_i^2(u)]E[G_j^2(v)] = 1 \times 1 \quad (4.26)$$

For  $i = j$ , the moment function is expanded via (7.28) of Ref. 12:

$$E[G_i^2(u)G_i^2(v)] = 1 + 2r^2(u-v) \quad (4.27)$$

where  $r(\ )$  is the autocovariance coefficient function for  $G_i(t)$ , all  $i$ . Substituting (4.26) and (4.27) in (4.25) yields

$$E[P(u)P(v)] = (pn^{-1})^2 \left\{ \sum_{i=1}^n \sum_{\substack{j=1 \\ i \neq j}}^n 1 + \sum_{i=1}^n [1 + 2r^2(u-v)] \right\} \quad (4.28)$$

Consolidating the first term in the single summand with the double sum gives

$$E[P(u)P(v)] = (pn^{-1})^2 [n^2 + 2nr^2(u-v)] \quad (4.29)$$

Then subtracting the square of the mean gives the autocovariance function of  $P(t)$ :

$$K_P(u-v) = 2p^2n^{-1}r^2(u-v) \quad (4.30)$$

Evaluating (4.30) for  $u = v$  and dividing by  $m_P$  gives the coefficient of variation:

$$c_P = \sigma_P \div m_P = \sqrt{2 \div n} \quad (4.31)$$

The sequence of values that can be assumed by  $c_P$  is  $\sqrt{2}$ , 1,  $\sqrt{2/3}$ ,  $\sqrt{1/2}$ ,  $\sqrt{2/5}$ , ... . For small values of  $n$ , the gaps between successive values of  $c_P$  are fairly large; therefore, it might not be possible to achieve an accurate approximation of a desired value of  $c_P$  by selecting the best value for  $n$ .

The third moment function for the power envelope process is

$$\begin{aligned} m_3(u,v,w) &= E[P(u)P(v)P(w)] \\ &= (p \div n)^3 \sum_{i=1}^n \sum_{j=1}^n \sum_{k=1}^n E[G_1^2(u)G_j^2(v)G_k^2(w)] \end{aligned} \quad (4.32)$$

The triple sum is decomposed according to the identity of the indices, and the expected values are evaluated via (7.28) of Ref. (12).

$$\begin{aligned}
 m_3(u,v,w) = (\rho \div n)^3 & \left\{ \sum_{i=1}^n \sum_{j=1}^n \sum_{k=1}^n 1 + \sum_{i=1}^n \sum_{k=1}^n [1 + 2r^2(u-w)] \right. \\
 & \quad \left. i \neq j \quad j \neq k \quad k \neq i \quad i \neq k \right. \\
 & + \sum_{i=1}^n \sum_{j=1}^n [1 + 2r^2(u-v)] + \sum_{j=1}^n \sum_{k=1}^n [1 + 2r^2(v-w)] \\
 & \quad \left. i \neq j \quad j \neq k \right. \\
 & + \sum_{i=1}^n [1 + 2r^2(u-v) + 2r^2(v-w) + 2r^2(w-u) + 8r(u-v)r(v-w)r(w-u)] \Big\}
 \end{aligned}
 \tag{4.33}$$

Consolidating the sums with the identical summands gives

$$\begin{aligned}
 m_3(u,v,w) = (\rho \div n)^3 & \left\{ n^3 + 2 \sum_{i=1}^n \sum_{j=1}^n [r^2(u-v) + r^2(v-w) + r^2(w-u)] \right. \\
 & + 8 \sum_{i=1}^n r(u-v)r(v-w)r(w-u) \Big\}
 \end{aligned}
 \tag{4.34}$$

The third joint central moment is

$$\begin{aligned}
 \mu_{1jk}(u,v,w) &= E\{[P_1(u) - m_1] [P_j(v) - m_j] [P_k(w) - m_k]\} \\
 &= m_{1jk}(u,v,w) - m_1 K_{jk}(v-w) - m_j K_{1j}(w-u) \\
 &\quad - m_k K_{1j}(u-v) - m_1 m_j m_k
 \end{aligned}
 \tag{4.35}$$



Substituting (4.24), (4.30) and (4.34) in (4.35) yields

$$\mu_3(u,v,w) = (2p)^3 n^{-2} r(u-v)r(v-w)r(w-u) \quad (4.36)$$

In some cases, estimates of the mean and autocovariance of the power envelope are available. The former can be used to obtain a value for  $p$  via (4.24), and the latter can be evaluated at  $u = v$  to obtain a value for  $n$  via (4.30). The autocovariance coefficient function can then be determined from (4.30). These elements determine the third central moment function for  $P(t)$  per (4.36).

The second power envelope process is also synthesized from squares of independent Gaussian processes. In this case, the weights in each term are not equal, and there are an infinite number of terms. The objective is to derive a non-negative process for which both mean and autocovariance can be specified. This objective is (generally) not met by the chi-square process, discussed previously.

The process is represented by

$$P(t) = p(1 - a) \sum_{i=0}^{\infty} a^i G_1^2(t) \quad (4.37)$$

where  $p > 0$  is a constant with dimensions of power

$0 \leq a < 1$  is a constant

$G_1(t)$  is a stationary Gaussian process with zero-mean and unit variance, statistically independent of  $G_j(t)$ ,  $j \neq 1$ .

It is clear from (4.37) and the stipulations above that  $P(t) \geq 0$ .

Given the properties of the Gaussian processes  $G_1(t)$  stated above the mean value of  $P(t)$  is

$$m_P = p(1 - a) \sum_{i=0}^{\infty} a^i \quad (4.38)$$

Since the indicated sum\* equals  $(1 - a)^{-1}$ , the result is

$$m_P = p \quad (4.39)$$

The second moment function of  $P(t)$  is

$$E[P(u)P(v)] = p^2 (1-a)^2 \sum_{i=0}^{\infty} \sum_{j=0}^{\infty} a^{i+j} E[G_1^2(u)G_j^2(v)] \quad (4.40)$$

For  $i \neq j$ , the fourth-order moment function in the summand is

$$E[G_1^2(u)] E[G_j^2(v)] = 1 \cdot 1 \quad (4.41)$$

For  $i = j$ , the moment function is expanded via (7.28) of Ref. (12):

$$E[G_1^2(u)G_1^2(v)] = 1 + 2r^2(u-v) \quad (4.42)$$

where  $r(u-v)$  is the autocovariance coefficient function for  $G_1(t)$ , all  $i$ . Substituting (4.42) and (4.41) in (4.40) yields

---

\*Ref. 13, 0.231, p. 7.

$$E[P(u)P(v)] = p^2(1-a^2) \left\{ \sum_{i=0}^{\infty} \sum_{\substack{j=0 \\ i \neq j}}^{\infty} a^{i+j} + \sum_{i=0}^{\infty} a^{2i} [1 + 2r^2(u-v)] \right\} \quad (4.43)$$

Consolidating the first term in the single summand with the double sum yields

$$E[P(u)P(v)] = p^2(1-a^2) \left\{ \left( \sum_{i=0}^{\infty} a^i \right)^2 + 2r^2(u-v) \sum_{i=0}^{\infty} a^{2i} \right\} \quad (4.44)$$

Then evaluating the sums via 0.231 No. 1 of Ref. 13 and cancelling common factors gives

$$E[P(u)P(v)] = p^2 \left[ 1 + 2 \frac{1-a}{1+a} r^2(u-v) \right] \quad (4.45)$$

Utilizing (4.45) and (4.39) gives the autocovariance function of  $P(t)$  as

$$K_P(u-v) = 2p^2 \frac{1-a}{1+a} r^2(u-v) \quad (4.46)$$

Evaluating the function for  $u = v$  gives the variance of  $P(t)$  as

$$\sigma_P^2 = 2p^2 (1-a)/(1+a) \quad (4.47)$$

Thus

$$K_P(u-v) = [\sigma_P r(u-v)]^2 \quad (4.48)$$

Using (4.47) and (4.39) gives the coefficient of variation as

$$c_P \equiv \sigma_P / m_P = \sqrt{2(1-a)/(1+a)} \quad (4.49)$$



It is seen that

$$\lim_{a \rightarrow 0} c_p = \sqrt{2} \quad (4.50)$$

and

$$\lim_{a \rightarrow 1} c_p = 0 \quad (4.51)$$

By selecting an appropriate value for the constant  $a$ , the coefficient of variation of  $P(t)$  can be any value between zero and  $\sqrt{2}$ . For  $a = 1$ , the sum has but one non-zero term; i.e., it is a chi-square process with one degree of freedom. And as  $a \rightarrow 1$ , the process becomes deterministic. Solving (4.49) for the constant  $a$  yields

$$a = \frac{2 - c_p^2}{2 + c_p^2} \quad (4.52)$$

Given the coefficient of variation  $c_p$  as a process parameter, the associated value of the parameter  $a$  can be determined. For the Kurtosis of the compound random process with the power envelope process given by (4.37), substituting (4.50) and (4.51) in (4.11) gives

$$\lim_{a \rightarrow 0} \mu_4 \div \sigma_p^4 = 9 \quad (4.53)$$

$$\lim_{a \rightarrow 1} \mu_4 \div \sigma_p^4 = 3 \quad (4.54)$$

For  $a \rightarrow 1$ , the compound process degenerates to a stationary Gaussian process.

The third moment function for the power envelope process is

$$m_3(u, v, w) = E[P(u)P(v)P(w)]$$

$$= p^3(1-a)^3 \sum_{i=0}^{\infty} \sum_{j=0}^{\infty} \sum_{k=0}^{\infty} a^{1+j+k} E[G_1^2(u)G_j^2(v)G_k^2(w)] \quad (4.55)$$

The triple sum is decomposed according to the identity of the indices, and the expected values are evaluated via (7.28) of Ref. (12).

$$m_3(u, v, w) = p^3(1-a)^3 \left\{ \sum_{\substack{i=0 \\ i \neq j}}^{\infty} \sum_{\substack{j=0 \\ j \neq k}}^{\infty} \sum_{\substack{k=0 \\ k \neq 1}}^{\infty} a^{1+j+k} + \sum_{\substack{i=0 \\ i \neq k}}^{\infty} \sum_{\substack{k=0 \\ k \neq 1}}^{\infty} a^{2i+k} [1 + 2r^2(u-w)] \right.$$

$$+ \sum_{\substack{i=0 \\ i \neq j}}^{\infty} \sum_{\substack{j=0 \\ j \neq k}}^{\infty} a^{1+2j} [1 + 2r^2(u-v)] + \sum_{\substack{j=0 \\ j \neq k}}^{\infty} \sum_{\substack{k=0 \\ k \neq 1}}^{\infty} a^{j+2k} [1 + 2r^2(v-w)]$$

$$\left. + \sum_{i=0}^{\infty} a^{3i} [1 + 2r^2(u-v) + 2r^2(v-w) + 2r^2(w-u) + 8r(u-v)r(v-w)r(w-u)] \right\} \quad (4.56)$$

Reconsolidating the sums with identical summands gives

$$\begin{aligned}
 m_3(u,v,w) = p^3(1-a)^3 & \left\{ \left( \sum_{i=0}^{\infty} a^i \right)^3 \right. \\
 & + 2 \sum_{i=0}^{\infty} a^i \sum_{j=0}^{\infty} a^{2j} [r^2(u-v) + r^2(v-w) + r^2(w-u)] \\
 & \left. + 8 \sum_{i=0}^{\infty} r(u-v)r(v-w)r(w-u) \right\} \quad (4.57)
 \end{aligned}$$

Evaluating the indicated sums via 0.231 No. 1 of Ref. (13) and cancelling common factors yields

$$\begin{aligned}
 m_3(u,v,w) = p^3 & \left\{ 1 + 2 \frac{1-a}{1+a} [r^2(u-v) + r^2(v-w) + r^2(w-u)] \right. \\
 & \left. + 8 \frac{(1-a)^3}{1-a^3} r(u-v)r(v-w)r(w-u) \right\} \quad (4.58)
 \end{aligned}$$

The third joint central moment is

$$\begin{aligned}
 \mu_{ijk}(u,v,w) & \equiv E\{[P_i(u) - m_i] [P_j(v) - m_j] [P_k(w) - m_k]\} \\
 & = m_3(u,v,w) - m_i K_{ij}(v-w) - m_j K_{ik}(w-u) \\
 & \quad - m_k K_{ij}(u-v) - m_i m_j m_k \quad (4.59)
 \end{aligned}$$



Substituting (4.58), (4.46), and (4.39) in (4.59) yields

$$\mu(u,v,w) = \beta p^3 r(u-v)r(v-w)r(w-u) \quad (4.60)$$

$$\text{where } \beta = [2(1-a)]^3 (1-a^3)^{-1}$$

In some cases, there are experimental data concerning the mean value and the autocovariance function for short-term average power, which approximates  $P(t)$ . These data can be used to establish a value for  $p$  via (4.39), a value for  $\sigma_p$  and the autocovariance function  $r(\ )$  via (4.48). From  $p$  and  $\sigma_p$  the value of the weighting parameter  $a$  is determined via (4.52). These elements determine the third central moment function per (4.60).

The process defined by (4.37) meets the objectives stated in the first paragraph of this section, with the limitation that the variance cannot be greater than twice the mean value.

Two power envelope processes have been proposed and analyzed. Given that parameter values are selected so that both have the same mean and variance, how are their third central moments related? If means and variances are equal, the coefficients of variation are equal. Equating expressions for the latter and solving gives  $a = (n-1) \div (n+1)$ . Substituting that result in (4.60) for  $u = v$  gives the third central moment for the WIS (weighted infinite sum) process in terms of the NCS (normalized chi-square) parameter  $n$ . Dividing that result into (4.36) evaluated at  $\mu = v$  and simplifying gives

$$\frac{\mu_3(\text{NCS})}{\mu_3(\text{WIS})} = \frac{3}{4} + \frac{1}{4n^2} \quad (4.61)$$

Except for the case  $n = 1$ , when the processes are identical, the WIS density is more skewed than that of the NCS.

A set of power envelope processes, some or all of which may be mutually dependent, can be synthesized from a set of independent power envelope processes:

$$P_1(t) = \sum_l a_{1l} Q_l(t) \quad (4.62)$$

where  $a_{1l} \geq 0$

$Q_l(t) \geq 0$ , and  $Q_m(t)$  is statistically independent of  $Q_l(t)$ ,  $m \neq l$ .

The mean value of  $P_1(t)$  is

$$p_1 = \sum_l a_{1l} m_l \quad (4.63)$$

where  $m_l = E[Q_l(t)]$

The joint second moment function is

$$R_{1j}(u-v) = E[P_1(t)P_j(t)] \quad (4.64)$$

Substituting (4.62) in (4.64) and evaluating gives

$$\begin{aligned} R_{1j}(u-v) &= \sum_m \sum_n a_{1m} a_{jn} E[Q_m(u)Q_n(v)] \\ &= \left( \sum_m a_{1m} m_m \right)^2 + \sum_m a_{1m} a_{jm} K_{Qm}(u-v) \end{aligned} \quad (4.65)$$

where  $K_{Q_m}(\ )$  is the autocovariance function for  $Q_m(t)$ . Utilizing (4.63) and (4.65) gives the cross-covariance function for  $P_i(u)$  and  $P_j(v)$ :

$$K_{ij}(u-v) = \sum_m a_{im} a_{jm} K_{Q_m}(u-v) \quad (4.66)$$

It is seen that the processes  $P_i(t)$  and  $P_j(t)$  will be dependent if  $a_{im} > 0$  and  $a_{jm} > 0$  for at least one value of the index  $m$ .

The third joint central moment function is evaluated by means of a similar procedure, and the result is

$$\mu_{ijk}(u,v,w) = \sum_m a_{im} a_{jm} a_{km} \mu_{Q_m}(u,v,w) \quad (4.67)$$

where  $\mu_{Q_m}(u,v,w)$  is the third central moment function for the power envelope process  $Q_m(t)$ .

If the basis processes are either of the types discussed previously in this section, then the cross-covariance function can be evaluated by substituting (4.48) in (4.66):

$$K_{ij}(u-v) = \sum_m a_{im} a_{jm} [\sigma_m r_m(u-v)]^2 \quad (4.68)$$

A similar procedure is followed to obtain the third joint central moment function.



$$\mu_{ijk}(u,v,w) = \sum_m a_{im} a_{jm} a_{km} \beta_m p_m^3 r_m(u-v) r_m(v-w) r_m(w-u) \quad (4.69)$$

where  $\beta_m = 2^3 n_m^{-2}$  for the envelope process defined by (4.23)

$$= [2(1-a_m)]^3 \div (1-a_m^3) \text{ for the envelope process defined by (4.37).}$$

## 5.0 EVALUATION OF OUTPUT MOMENTS

Section 3.0 established the need for calculating the moments of the test statistic. The moments of the test statistic to order three will be evaluated for the case in which the inputs to the multichannel analog are compound random processes of the type described in Section 4.0.

The moments are obtained by deriving the expected values of the appropriate powers of the test statistic as given by (2.9), which can be expressed in more compact form as

$$Z = T^{-1} \int_0^T du \left[ 2N_S(u)N_0(u) - \sum_{i=S}^n c_i N_1^2(u) \right] \quad (5.1)$$

where  $N_S(t) \equiv S(t)$ ,  $c_S = -1$ , and the indices in the sum are  $S, 0, 1, 2, 3, \dots, n$ .

The first moment or mean value of the test statistic is the expected value of (5.1):

$$m_Z = T^{-1} \int_0^T du \left\{ 2E[N_S(u)N_0(u)] - \sum_{i=S}^n c_i E[N_1^2(u)] \right\} \quad (5.2)$$

The first term of the integrand is zero per (4.19), and the components of the indicated sum are evaluated per (4.22). Evaluation of the integral then yields

$$m_Z = - \sum_{i=S}^n c_i p_i \quad (5.3)$$

The second moment is the expected value of the square of (5.1), which can be expressed as:

$$Z^2 = T^{-2} \int_0^T du \int_0^T dv \left[ 4N_S(u)N_S(v)N_0(u)N_0(v) - 4N_S(u)N_0(u) \sum_S^n e_i N_1^2(v) + \sum_S^n \sum_S^n c_i c_j N_1^2(u)N_j^2(v) \right] \quad (5.4)$$

If the first term of the integrand is expressed in terms of (4.18), its expected value is

$$E(T_1) = 4E \left[ \sqrt{P_S(u)P_S(v)P_0(u)P_0(v)} \right] E[G_S(u)G_S(v)] E[G_0(u)G_0(v)] \quad (5.5)$$

and if the relaxation time of the P-processes is much longer than those of the G-processes, then

$$E(T_1) \approx 4p_S p_0 \rho_S(u-v) \rho_0(u-v) \quad (5.6)$$

If the second term of the integrand is expressed in terms of (4.18), its expected value can be expressed as

$$E(T_2) = -4 \sum_{i=S}^n E \left[ \sqrt{P_S(u)P_0(u)P_1^2(v)} \right] E[G_S(u)G_0(u)G_1^2(v)] \quad (5.7)$$

For  $i=S$ , the second expected value is  $E[G_S(u)G_S^2(v)] E[G_0(u)]$ , which is zero since the second factor is zero. For  $i=0$ , the second expected value is  $E[G_S(u)] E[G_0(u)G_0^2(v)]$ , which is zero



because the first factor is zero. And for  $i = 1, 2, \dots, n$ , the second expected value is  $E[G_S(u)] E[G_0(u)] E[G_1^2(v)]$ , which also equals zero. Thus

$$E(T_2) = 0 \quad (5.8)$$

The third term of the integrand of (5.4) is expressed as a double summation. For  $i \neq j$ ,

$$\begin{aligned} E[N_1^2(u)N_j^2(v)] &= E[P_1(u)P_j(v)] E[Q_1^2(u)] E[Q_j^2(v)] \\ &= p_1 p_j + K_{1j}(u-v) \end{aligned} \quad (5.9)$$

since both the second and third factors are unity. For terms such that  $i = j$

$$E[N_1^2(u)N_1^2(v)] = E[P_1(u)P_1(v)] E[Q_1^2(u)Q_1^2(v)] \quad (5.10)$$

The second factor, a fourth moment function of a Gaussian process, is evaluated by means of (7.28) of Ref. 12. Thus

$$E[N_1^2(u)N_1^2(v)] = [p_1^2 + K_{11}(u-v)] [1 + 2\rho^2(u-v)] \quad (5.11)$$

$$= p_1^2 + K_{11}(u-v) + 2(p_1^2 + \sigma_1^2)\rho^2(u-v) \quad (5.12)$$

Utilizing (5.9) and (5.12) permits the evaluation of the expected value of the third term of the integrand:

$$\begin{aligned} E(T_3) &= \sum_{i=1}^n \sum_{j=1}^n c_i c_j [p_i p_j + K_{ij}(u-v)] + 2 \sum_{i=1}^n c_i^2 (p_i^2 + \sigma_i^2) \rho^2(u-v) \\ &\quad (5.13) \end{aligned}$$

The variance of the test statistic is the expected value of its square less the square of its mean value. Utilization of (5.13), (5.8), (5.6), and (5.3) gives

$$\sigma_Z^2 = T^{-2} \int_0^T du \int_0^T dv \left[ 4p_S p_0 \rho_S(u-v) \rho_0(u-v) + 2 \sum_{i=S}^n c_i^2 (p_i^2 + \sigma_i^2) \rho_i^2(u-v) + \sum_{i=S}^n \sum_{j=S}^n c_i c_j K_{ij}(u-v) \right] \quad (5.14)$$

If the variables of integration are changed to  $x = u + v$  and  $y = u - v$ , the result can be expressed as

$$\sigma_Z^2 = T^{-1} \int_{-T}^T dy \left[ 4p_S p_0 \rho_S(y) \rho_0(y) + 2 \sum_{i=S}^n c_i^2 (p_i^2 + \sigma_i^2) \rho_i^2(y) + \sum_{i=S}^n \sum_{j=S}^n c_i c_j K_{ij}(y) \right] (1 - |y|T^{-1}) \quad (5.15)$$

If the decay times of the functions  $\rho_i(y)$  are very small compared to the integration period  $T$ , then

$$\sigma_Z^2 \approx 2T^{-1} \int_{-\infty}^{\infty} dy \left[ 2p_S p_0 \rho_S(y) \rho_0(y) + \sum_{i=S}^n c_i^2 (p_i^2 + \sigma_i^2) \rho_i^2(y) \right] + T^{-1} \int_{-T}^T dy (1 - |y|T^{-1}) \sum_{i=S}^n \sum_{j=S}^n c_i c_j K_{ij}(y) \quad (5.16)$$

$$= T^{-1} \left[ 2p_S p_0 W_{S0}^{-1} + \sum_{i=S}^n c_i^2 (p_i^2 + \sigma_i^2) W_{ii}^{-1} \right] + T^{-1} \int_{-T}^T dy (1 - |y|T^{-1}) \sum_{i=S}^n \sum_{j=S}^n c_i c_j K_{ij}(y) \quad (5.17)$$

where  $W_{1j}^{-1} \equiv 2 \int_{-\infty}^{\infty} dy \rho_1(y) \rho_j(y)$  can be considered as the reciprocal of the joint equivalent bandwidth of the associated random processes.

The third moment of the test statistic is the expected value of the cube of the test statistic, which can be expressed as

$$\begin{aligned}
 Z^3 = T^{-3} \int_0^T du \int_0^T dv \int_0^T dw & \left[ 8N_S(u)N_S(v)N_S(w)N_0(u)N_0(v)N_0(w) \right. \\
 & - 12N_S(u)N_S(v)N_0(u)N_0(v) \sum_{i=S}^n c_i N_i^2(w) \\
 & + 6N_S(u)N_0(u) \sum_{i=S}^n \sum_{j=S}^n c_i c_j N_i^2(v)N_j^2(w) \\
 & \left. - \sum_{i=S}^n \sum_{j=S}^n \sum_{k=S}^n c_i c_j c_k N_i^2(u)N_j^2(v)N_k^2(w) \right] \quad (5.18)
 \end{aligned}$$

If the first term of the integrand is expressed in terms of (4.18), its expected value is

$$\begin{aligned}
 E(U_1) = 8E & \left[ \sqrt{P_S(u)P_S(v)P_S(w)P_0(u)P_0(v)P_0(w)} \right] \\
 & \times E[G_S(u)G_S(v)G_S(w)] E[G_0(u)G_0(v)G_0(w)] \quad (5.19)
 \end{aligned}$$

According to (7.28) of Ref. 12, the second and third factors are zero; thus

$$E(U_1) = 0 \quad (5.20)$$



If the second term of the integrand of (5.18) is expressed in terms of (4.18) and then partially expanded, its expected value is

$$\begin{aligned}
 E(U_2) = 12 \Big\{ & E \left[ \sqrt{P_S(u)P_S(v)P_S^2(w)P_0(u)P_0(v)} \right] \\
 & \times E[G_S(u)G_S(v)G_S^2(w)] E[G_0(u)G_0(v)] \\
 & + E \left[ \sqrt{P_S(u)P_S(v)P_0(u)P_0(v)P_0^2(w)} \right] \\
 & \times E[G_S(u)G_S(v)] E[G_0(u)G_0(v)G_0^2(w)] \\
 & - \sum_{i=1}^n c_i E \left[ \sqrt{P_S(u)P_S(v)P_0(u)P_0(v)P_i^2(w)} \right] \\
 & \times E[G_S(u)G_S(v)] E[G_0(u)G_0(v)] E[G_i^2(w)] \Big\} \quad (5.21)
 \end{aligned}$$

Applying (7.28) of Ref. 12 yields

$$\begin{aligned}
 E(U_2) = 12 \Big\{ & E \left[ \sqrt{P_S(u)P_S(v)P_0(u)P_0(v)P_S^2(w)} \right] \\
 & \times \rho_0(u-v) [\rho_S(u-v) + 2\rho_S(w-u)\rho_S(v-w)] \\
 & + E \left[ \sqrt{P_S(u)P_S(v)P_0(u)P_0(v)P_0^2(w)} \right] \\
 & \times \rho_S(u-v) [\rho_0(u-v) + 2\rho_0(w-u)\rho_0(v-w)] \\
 & - \sum_{i=1}^n c_i E \left[ \sqrt{P_S(u)P_S(v)P_0(u)P_0(v)P_i^2(w)} \right] \\
 & \times \rho_S(u-v)\rho_0(u-v) \Big\} \quad (5.22)
 \end{aligned}$$

Combining the first, third, and fifth terms gives

$$\begin{aligned}
 E(U_2) = 12 \bigg\{ & 2E \left[ \sqrt{P_S(u)P_S(v)P_0(u)P_0(v)P_S^2(w)} \right] \\
 & \rho_0(u-v)\rho_S(w-u)\rho_S(v-w) \\
 & + 2E \left[ \sqrt{P_S(u)P_S(v)P_0(u)P_0(v)P_0^2(w)} \right] \\
 & \times \rho_S(u-v)\rho_0(w-u)\rho_0(v-w) \\
 & - \sum_{i=S}^n c_i E \left[ \sqrt{P_S(u)P_S(v)P_0(u)P_0(v)P_i^2(w)} \right] \\
 & \times \rho_S(u-v)\rho_0(u-v) \bigg\} \quad (5.23)
 \end{aligned}$$

If the relaxation times of the P-processes are much longer than those of the G-processes,

$$\begin{aligned}
 E(U_2) = 12 \bigg\{ & 2E \left[ P_S^2(w)P_0(w) \right] \rho_S(v-w)\rho_S(w-u)\rho_0(u-v) \\
 & + 2E \left[ P_S(w)P_0^2(w) \right] \rho_S(u-v)\rho_0(v-w)\rho_0(w-u) \\
 & - \sum_{i=S}^n c_i E \left[ P_S(u)P_0(u)P_i(w) \right] \rho_S(u-v)\rho_0(u-v) \bigg\} \quad (5.24)
 \end{aligned}$$

If the third term of the integrand of (5.18) is expressed in terms of (4.18), its expected value is

$$E(U_3) = 6 \sum_{i=S}^n \sum_{j=S}^n c_i c_j E \left[ \sqrt{P_S(u) P_0(u) P_1(v) P_j(w)} \right] \\ \times E \left[ G_S(u) G_0(u) G_1^2(v) G_j^2(w) \right] \quad (5.25)$$

For terms in which neither  $i$  nor  $j$  is equal to  $S$  or  $0$ , the second expected value is  $E[G_S(u)]E[G_0(u)]E[G_1^2(v)G_j^2(w)] = 0$ . For  $i = j = S$ , and for  $i = j = 0$ , the second expected value in (5.25) is also zero. Finally, for  $i = S$  and  $j = 0$  and vice versa, the second expected value is also zero. Thus

$$E(U_3) = 0. \quad (5.26)$$

The fourth term of the integrand of (5.18) is represented as a triple sum. Within this sum there are  $n + 2$  terms with  $i = j = k$ . The expected value of the sum of those terms can be represented as

$$E(U_{41}) = - \sum_{i=S}^n c_i^3 E \left[ P_1(u) P_1(v) P_1(w) \right] E \left[ G_1^2(u) G_1^2(v) G_1^2(w) \right] \quad (5.27)$$

Applying (7.28) of Ref. 12 to the second expected value gives

$$E(U_{41}) = - \sum_{i=S}^n c_i^3 E \left[ P_1(u) P_1(v) P_1(w) \right] \left[ 1 + 2\rho_1^2(u-v) \right. \\ \left. + 2\rho_1^2(v-w) + 2\rho_1^2(w-u) + 8\rho_1(u-v)\rho_1(v-w)\rho_1(w-u) \right] \quad (5.28)$$

In the triple sum there are  $3(n+2)(n+1)$  terms in which two of the indices are equal but different from the third. After application of (7.28) of Ref. 12, the expected value of the sum of those terms can be represented as



$$\begin{aligned}
E(U_{42}) = & - \sum_{i=S}^n \sum_{\substack{j=S \\ j \neq i}}^n c_i^2 c_j \left\{ E \left[ P_1(u) P_1(v) P_j(w) \right] \left[ 1 + 2\rho_1^2(u-v) \right] \right. \\
& + E \left[ P_j(u) P_1(v) P_1(w) \right] \left[ 1 + 2\rho_1^2(v-w) \right] \\
& \left. + E \left[ P_1(u) P_j(v) P_1(w) \right] \left[ 1 + 2\rho_1^2(w-u) \right] \right\} \quad (5.29)
\end{aligned}$$

In the triple sum there are  $(n+2)(n+1)n$  terms with all of the summation indices different. The expected value of the sum of these terms can be represented as

$$\begin{aligned}
E(U_{43}) = & - \sum_{i=S}^n \sum_{\substack{j=S \\ j \neq i}}^n \sum_{\substack{k=S \\ k \neq i, j}}^n c_i c_j c_k E \left[ P_1(u) P_j(v) P_k(w) \right] \quad (5.30)
\end{aligned}$$

Summing (5.28) through (5.30) gives the expected value of the fourth term of the integrand of (5.18):

$$\begin{aligned}
E(U_4) = & - \sum_{i=S}^n \sum_{j=S}^n \sum_{k=S}^n c_i c_j c_k E \left[ P_1(u) P_j(v) P_k(w) \right] \\
& - 2 \sum_{i=S}^n \sum_{j=S}^n c_i^2 c_j \left\{ E \left[ P_1(u) P_1(v) P_j(w) \right] \rho_1^2(u-v) \right. \\
& + E \left[ P_j(u) P_1(v) P_1(w) \right] \rho_1^2(v-w) + E \left[ P_1(u) P_j(v) P_1(w) \right] \rho_1^2(w-u) \left. \right\} \\
& - 8 \sum_{i=S}^n c_i^3 E \left[ P_1(u) P_1(v) P_1(w) \right] \rho_1(u-v) \rho_1(v-w) \rho_1(w-u) \quad (5.31)
\end{aligned}$$

Expressions (5.24) and (5.31) give the expected values of the terms of the integrand of (5.18). Given the symmetry of certain of the integrands, the expected value of the cube of the test statistic can be expressed as

$$\begin{aligned}
 E(Z^3) = T^{-3} \int_0^T du \int_0^T dv \int_0^T dw \bigg\{ & 24E[P_S^2(w)P_0(w)] \rho_S(v-w)\rho_S(w-u)\rho_0(u-v) \\
 & + 24E[P_S(w)P_0^2(w)] \rho_S(u-v)\rho_0(v-w)\rho_0(w-u) \\
 & - 12 \sum_{i=S}^n c_i E[P_S(u)P_0(u)P_1(w)] \rho_S(u-v)\rho_0(u-v) \\
 & - 8 \sum_{i=S}^n c_i^3 E[P_1(u)P_1(v)P_1(w)] \rho_1(u-v)\rho_1(v-w)\rho_1(w-u) \\
 & - 6 \sum_{i=S}^n \sum_{j=S}^n c_i^2 c_j E[P_1(u)P_1(v)P_j(w)] \rho_1^2(u-v) \\
 & - \sum_{i=S}^n \sum_{j=S}^n \sum_{k=S}^n c_i c_j c_k E[P_1(u)P_j(v)P_k(w)] \bigg\} \quad (5.32)
 \end{aligned}$$

The third central moment of the test statistic is

$$\begin{aligned}
 \mu_{3Z} &= E(Z - m_Z)^3 \\
 &= E(Z^3) - 3m_Z \sigma_Z^2 - m_Z^3 \quad (5.33)
 \end{aligned}$$

The third moment functions appearing in the integrand can be expressed in terms of central moment functions. The most general of these is

$$\begin{aligned}
& E[P_1(u)P_j(v)P_k(w)] \\
&= E\left\{\left[P_1(u) - p_1 + p_1\right]\left[P_j(v) - p_j + p_j\right]\left[P_k(w) - p_k + p_k\right]\right\} \\
&= \mu_{1jk}(u-v, v-w, w-u) + p_1 K_{jk}(v-w) + p_j K_{k1}(w-u) \\
&\quad + p_k K_{1j}(u-v) + p_1 p_j p_k \tag{5.34}
\end{aligned}$$

where  $\mu_{1jk}(u-v, v-w, w-u) = E\{[P_1(u) - p_1][P_j(v) - p_j][P_k(w) - p_k]\}$ .

The expression for  $E(Z^3)$  is expanded by evaluating (5.34) for the various terms of (5.32). The expanded result is substituted in (5.33), along with (5.3) and (5.14) to obtain the third central moment of the test statistic, shown in Table 1.

Table 1. Third Central Moment of Test Statistic

$$\begin{aligned}
\mu_{3Z} = T^{-3} \int_0^T du \int_0^T dv \int_0^T dw \bigg\{ & 24 \left[ \mu_{SS0} + 2P_S \sigma_{S0}^2 + p_0(p_S^2 + \sigma_S^2) \right] \rho_S(v-w) \rho_S(w-u) \rho_0(u-v) \\
& + 24 \left[ \mu_{S00} + 2p_0 \sigma_{S0}^2 + p_S(p_0^2 + \sigma_0^2) \right] \rho_S(u-v) \rho_0(v-w) \rho_0(w-u) \\
& - 12 \sum_{i=S}^n c_i \left[ \mu_{S0i}(0, u-w, w-u) + p_S K_{0i}(u-w) + p_0 K_{Si}(w-u) + p_i \sigma_{S0}^2 \right] \rho_S(u-v) \rho_0(u-v) \\
& - 8 \sum_{i=S}^n c_i^3 \left[ \mu_{3i} + 3p_i \sigma_i^2 + p_i^3 \right] \rho_i(u-v) \rho_i(v-w) \rho_i(w-u) \\
& - 6 \sum_{i=S}^n \sum_{j=S}^n c_i^2 c_j \left[ \mu_{i1j}(0, u-w, w-u) + 2p_i K_{1j}(u-w) \right] \rho_i^2(u-v) \\
& \quad - \sum_{i=S}^n \sum_{j=S}^n \sum_{k=S}^n c_i c_j c_k \mu_{ijk}(u-v, v-w, w-u) \bigg\}
\end{aligned}$$



The first, second, and fourth lines in Table 1 are represented by an integral of the form

$$I = T^{-3} \int_{-T/2}^{T/2} du \int_{-T/2}^{T/2} dv \int_{-T/2}^{T/2} dw r(u-v)s(v-w)t(w-u) \quad (5.35)$$

A change of variables  $x = w-u$  and  $y = w+u$  yields, for half of the domain of integration

$$I_+ = \frac{1}{2} T^{-3} \int_{-T/2}^{T/2} dv \int_0^T dx t(x) \int_{-T+x}^{T-x} dy r(y/2-x/2-v)s(v-y/2-x/2) \quad (5.36)$$

which equals the result from the other half of the domain of integration, given that all of the functions have even symmetry. If the decay time of  $t(x)$  is small compared to the integration period  $T$ , then

$$I = 2I_+ \approx T^{-3} \int_{-T/2}^{T/2} dv \int_0^T dx t(x) \int_{-T}^T dy r(y/2-x/2-v)s(v-y/2-x/2) \quad (5.37)$$

If the functions  $r(\ )$  and  $s(\ )$  are represented as the inverse Fourier transforms of  $R(\ )$  and  $S(\ )$  respectively, then, after some algebraic manipulation,

$$I = T^{-3} \int_{-\infty}^{\infty} df R(f) \int_{-\infty}^{\infty} dg S(g) \int_{-T/2}^{\infty} dv \exp 2\pi j(g-f)v \\ \times \int_0^T dx t(x) \exp [-\pi j(f+g)x] \int_{-T}^T dy \exp \pi j(f-g)y \quad (5.38)$$

If the decay time of  $t(\ )$  is small compared to  $T$ , then the fourth integral of (5.38) is approximately  $\frac{1}{2}T(\frac{f+g}{2})$ , where  $T(\ )$  is the Fourier transform of  $t(\ )$ . Substituting this result in (5.38) and evaluating the  $v$  and  $y$  integrals yields

$$I = T^{-1} \int_{-\infty}^{\infty} df R(f) \int_{-\infty}^{\infty} dg S(g) T\left(\frac{f+g}{2}\right) \left(\frac{\sin \pi(g-f)T}{(g-f)T}\right)^2 \quad (5.39)$$

A change of variables  $h = g - f$  in the second integral yields

$$I = T^{-1} \int_{-\infty}^{\infty} df R(f) \int_{-\infty}^{\infty} dh S(h+f) T\left(\frac{h}{2}+f\right) \left(\frac{\sin \pi hT}{\pi hT}\right)^2 \quad (5.40)$$

If the averaging time  $T$  is large, then the last factor is very small except in a small increment around  $h = 0$ . If  $S(\ )$  and  $T(\ )$  are bandpass functions, then  $f \gg h$  over the bandpasses, and

$$I \approx T^{-1} \int_{-\infty}^{\infty} df R(f) S(f) T(f) \int_{-\infty}^{\infty} dh \left(\frac{\sin \pi hT}{\pi hT}\right)^2 \quad (5.41)$$

The  $h$ -integral, evaluated via 3.821, number 9 of Ref. 13, equals  $T^{-1}$ ; thus

$$I \approx T^{-1} \int_{-\infty}^{\infty} df R(f) S(f) T(f) \quad (5.42)$$

Since the spectral functions in (5.42) are Fourier transforms of autocovariance coefficients, the dimension of the integral in (5.42) is  $1 \div \text{frequency squared}$ . Let

$$W_{\text{rft}}^{-2} = 4 \int_{-\infty}^{\infty} df R(f) S(f) T(f) \quad (5.43)$$

If all of the spectra have coincident rectangular bandpasses of width  $W$ , then  $W_{\text{rft}} = W$ . Utilizing (5.43) in (5.42) gives

$$I = \left( 2TW_{\text{rft}} \right)^{-2} \quad (5.44)$$

The third and fifth lines of Table 1 include integrals of the form

$$I = T^{-3} \int_{-T/2}^{T/2} du \int_{-T/2}^{T/2} dv \int_{-T/2}^{T/2} dw f(u-w)r(u-v)s(u-v) \quad (5.45)$$

where the decay times of  $r( )$  and  $s( )$  are much smaller than that of  $f( )$ , and much smaller than the length of the integration period  $T$ . A change of variables  $x = u-v$  and  $y = u+v$  yields, for half of the domain of integration,

$$I + = \frac{1}{2} T^{-3} \int_0^T dx r(x)s(x) \int_{-T/2}^{T/2} dw \int_{-T+x}^{T/2} dy f(x/2+y/2-w) \quad (5.46)$$

which equals the result from the other half of the domain of integration. Given the stipulations stated above

$$I = 2I + = T^{-3} \int_0^T dx r(x)s(x) \int_{-T/2}^{T/2} dw \int_{-T}^T dy f(y/2-w) \quad (5.47)$$



A change of variables to  $p = y/2 - w$  and  $q = y/2 + w$  gives, for half of the domain of integration

$$I_p = T^{-3} \int_0^T dx r(x)s(x) \int_0^T dp f(p) \int_{-T+p}^{T-p} dq, \quad (5.48)$$

which equals the result from the other half of the domain. Evaluating the  $q$  integral yields

$$I = 2I_p = 4T^{-2} \int_0^T dx r(x)s(x) \int_0^T dp f(p) (1 - pT^{-1}) \quad (5.49)$$

Given the stipulations stated above,

$$I \approx 2T^{-2} \int_{-\infty}^{\infty} dx r(x)s(x) \int_0^T dp f(p) (1 - pT^{-1}) \quad (5.50)$$

$$= \left(2T^2 W_{rs}\right)^{-1} \int_{-T}^T dp f(p) (1 - |p|T^{-1}) \quad (5.51)$$

where the joint equivalent bandwidth is defined below (5.17).

Application of (5.46) and (5.51) to the expression in Table 1 yields the result in Table 2.

The last term of the expression in Table 2 includes a triple integral whose integrand is the joint third central moment function of the power envelope processes. This integral can be partially evaluated for the power envelope processes defined by (4.23) and (4.37). For those processes, the joint third central moment function

Table 2. Evaluation of Third Central Moment

$$\begin{aligned}
\mu_{3Z} = T^{-2} \bigg\{ & 6 W_{SS0}^{-2} \left[ \mu_{SS0} + 2p_S \sigma_S^2 + p_0(p_S^2 + \sigma_S^2) \right] \\
& + 6 W_{S00}^{-2} \left[ \mu_{S00} + 2p_0 \sigma_{S0}^2 + p_S(p_0^2 + \sigma_0^2) \right] \\
& - 6 W_{S0}^{-1} \sum_{i=S}^n c_i \int_{-T}^T du \left[ \mu_{S0i}(0, u, u) + p_S K_{0i}(u) + p_0 K_{Si}(u) + p_i \sigma_{S0}^2 \right] (1 - |u|T^{-1}) \\
& - 2 \sum_{i=S}^n c_i^3 W_{iii}^{-2} \left[ \mu_{3i} + 3p_i \sigma_i^2 + p_i^3 \right] \\
& - 3 \sum_{i=S}^n \sum_{j=S}^n c_i^2 c_j W_{ij}^{-1} \int_{-T}^T du \left[ \mu_{ij}(0, u, u) + 2p_i K_{ij}(u) \right] (1 - |u|T^{-1}) \bigg\} \\
& - T^{-3} \sum_{i=S}^n \sum_{j=S}^n \sum_{k=S}^n c_i c_j c_k \int_0^T \int_0^T \int_0^T dv \int dw \mu_{ijk}(u-v, v-w, w-u)
\end{aligned}$$

is given by (4.36) and (4.60) respectively; for either case, the essential integral can be represented by

$$I = \int_0^T du \int_0^T dv \int_0^T dw r(u-v)s(v-w)t(w-u) \quad (5.52)$$

A new set of variables is defined by the transformations

$$\begin{aligned} u &= x - z & x &= -v + w \\ v &= y - z & y &= -u + w \\ w &= x + y - z & z &= -u - v + w \end{aligned} \quad (5.53)$$

With the change of variables, the integral is

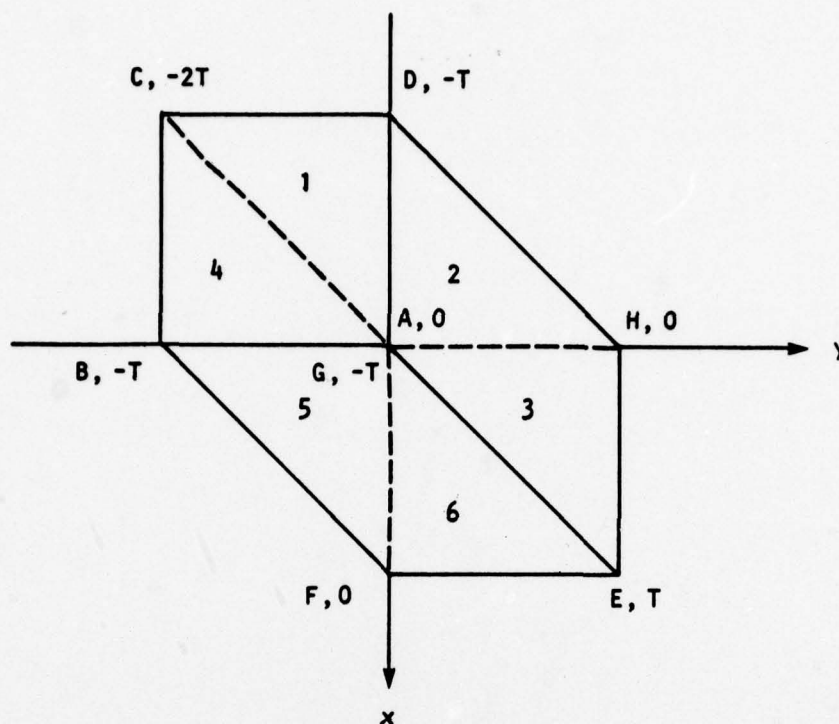
$$I = \int_R dx \int dy \int dz r(x-y)r(-x)r(y) \quad (5.54)$$

The region of integration is a three-dimensional polygon. Figure 5.1 shows a plan view of the polygon in the x-y plane. The z-coordinate of each vertex is indicated. The figure also gives the equations of the faces of the polygon. The region of integration is divided into six parts numbered as shown.

Part 1 of the region is bounded above by the face ABCD and below by the face CDHG. It is also bounded by the plane  $x=y$ , and  $y=0$ . The integral for this part is therefore

$$I_1 = \int_{-T}^0 dx \int_x^0 dy r(x-y)r(-x)r(y) \int_{-T+y}^{x+y} dz \quad (5.55)$$





<u>FACE</u>	<u>EQUATION</u>
A B C D	$z = x + y$
E F G H	$z = -T + x + y$
A B F E	$z = y$
B C G F	$z = -T + x$
C D H G	$z = -T + y$
A D H E	$z = x$

FIGURE 5.1 Plan View of Polygon.

$$= \int_{-T}^0 dx \int_x^0 dy r(x-y)r(-x)r(y)(T+x) \quad (5.56)$$

An alternative form is found by changing the signs of the variables of integration:

$$I_1 = \int_0^T dx \int_0^x dy r(-x+y)r(x)r(-y)(T-x) \quad (5.57)$$

Part 2 of the region is bounded above by the face ADHE and below by DCHG. It is also bounded by the planes  $y=0$  and  $x=0$ . The integral for this part is

$$I_2 = \int_0^T dy \int_0^{-T+y} dx r(x-y)r(-x)r(y) \int_{-T+y}^x dz \quad (5.58)$$

$$= \int_0^T dy \int_0^{-T+y} dx r(x-y)r(-x)r(y)(T+x-y) \quad (5.59)$$

Now let  $w = -x+y$  in the inner integral:

$$I_2 = \int_0^T dy \int_y^T dw r(-w)r(w-y)r(y)(T-w) \quad (5.60)$$

Interchanging the order of integration then gives

$$I_2 = \int_0^T dw \int_0^w dy r(-w)r(w-y)r(y)(T-2) \quad (5.61)$$

The function  $r(\ )$  is the autocovariance coefficient function for the Gaussian processes that are the components of the power envelope processes described in Section 4.3; thus, it is an even function of its argument, and comparing (5.61) to (5.57) shows that  $I_2 = I_1$ .

Part 3 of the region is bounded above by the face ADHE and below by EFGH. It is also bounded by the planes  $x = 0$ , and  $x = y$ . The integral for this part is

$$I_3 = \int_0^T dy \int_0^y dx r(x-y)r(-x)r(y) \int_{-T+x+y}^x dz \quad (5.62)$$

$$= \int_0^T dy \int_0^y dx r(x-y)r(-x)r(y)(T-y) \quad (5.63)$$

Interchanging the variables of integration in (5.63) and comparing the result to (5.57) for  $I$ , shows that  $I_3 = I_1$ .

The integrals for Parts 4, 5, and 6 of the region of integration are identical to those of Parts 1, 2, and 3, respectively. Since the latter trio are all equal the complete result may be expressed by

$$I = 6 \int_0^T dx r(x)(T-x) \int_0^x dy r(x-y)r(y) \quad (5.64)$$

Substituting this result into the sixth term of the expression in Table 2 gives



$$T_6 = - \sum_m \beta_m p_m^3 I_m \sum_{i=S}^n \sum_{j=S}^n \sum_{k=S}^n c_{i1} a_{im} c_{j1} a_{jm} c_{k1} a_{km} \quad (5.65)$$

$$\text{where } I_m = 6 T^{-2} \int_0^T dx r_m(x) (1-xT^{-1}) \int_0^x dy r_m(x-y) r_m(y)$$

The results of this section are low-order moments of the test statistic  $Z$  of the channel of interest. The results include (5.3) for the mean value, (5.17) for the variance, Table 2 for the third central moment, and (5.65) for a partial evaluation of the sixth term in Table 2.

## 6.0 TIME-INVARIANT POWER ENVELOPES

This section considers two cases in which the power envelopes are time-invariant.

In the first case, the envelopes are deterministic constants, and the input processes are therefore Gaussian. This case is analyzed to establish a set of values for the weighting coefficients of the multichannel analog.

In the second case, the envelopes are random variables, and the input processes are therefore only conditionally Gaussian on the random variables. This case is analyzed to establish the conditions for the applicability of a formula that has been employed to calculate the probability of detection in an environment with fluctuating sonar parameters.

### 6.1 Special Case: $P_i(t) = p_N$

In many analyses of passive sonar receiver performance, it is assumed that both the signal and the noise in a single channel are zero-mean statistically independent Gaussian processes. For the analysis of this section it will further be assumed that the noise processes of the other channels are zero-mean statistically independent Gaussian processes, all statistically identical. This is a degenerate case of the compound process of Section 4.0 in which

$$P_S(t) = p_S \quad (6.1)$$

$$P_i(t) = p_N, \quad i = 0, 1, 2, \dots, n \quad (6.2)$$

where  $p_S$  and  $p_N$  are constants. The results of this case will be used to establish a set of values for the threshold weighting coefficients  $c_i$ ,  $i = 1, 2, 3, \dots, n$ .

The mean value of the test statistic for this case is found by substituting (6.1) and (6.2) in (5.3):

$$m_Z = p_S + p_N \left( 1 - \sum_{i=1}^n c_i \right) \quad (6.3)$$

The variance of the test statistic is found by substituting (6.1) and (6.2) in (5.17):

$$\sigma_Z^2 = (WT)^{-1} \left[ p_S^2 + 2p_S p_N + p_N^2 \left( 1 + \sum_{i=1}^n c_i^2 \right) \right] \quad (6.4)$$

In this step, it was assumed that the equivalent bandwidth of the signal is identical to those of the noise processes.

The probabilities of detection and false alarm are given by (2.13) and (2.14) respectively, which show that both of these probabilities depend on the coefficient of variation  $c_Z \equiv \sigma_Z / m_Z$  of the test statistic. The inverse of that coefficient for the case of signal present is found by dividing (6.3) by the square root of (6.4):

$$\frac{1}{c_Z} = \sqrt{WT} \frac{r + 1 - \sum_{i=1}^n c_i}{\sqrt{r^2 + 2r + 1 + \sum_{i=1}^n c_i^2}} \quad (6.5)$$



where  $r = p_S \div p_N$  is the signal-to-noise power ratio. For the case of noise alone,

$$\frac{1}{c_Z} = \sqrt{WT} \frac{1 - \sum_{i=1}^n c_i}{\sqrt{1 + \sum_{i=1}^n c_i^2}} \quad (6.6)$$

This result is independent of the noise power  $p_N$ .

The weighting coefficients will be selected to maximize the detection probability while achieving a specified false alarm probability. If the time-bandwidth product is very large, then the test statistic is nearly normal, and the form of the density function for the standardized variable  $(Z - m_Z) \div \sigma_Z$  is very insensitive to the choice of weighting coefficients. Then the probabilities of detection and false alarm depend almost entirely on the coefficient of variation of the test statistic. To achieve a specified probability of false alarm,

$$1/c_Z = -\gamma \quad (6.7)$$

where  $\gamma$  is a positive constant. Substituting (6.7) in (6.6) and solving gives

$$\sqrt{WT} \left( 1 - \sum_{i=1}^n c_i \right) = -\gamma \sqrt{1 + \sum_{i=1}^n c_i^2} \quad (6.8)$$

and substituting this result in (6.5) gives

$$\frac{1}{c_Z} = \frac{\sqrt{WT} r - \gamma q}{\sqrt{r^2 + 2r + q^2}} \quad (6.9)$$

where

$$q = \sqrt{1 + \sum_{i=1}^n c_i^2} \quad (6.10)$$

It is clear from (2.13) that the probability of detection increases with the ratio  $1/c_Z$ . By differentiating (6.9) with respect to  $q$  it is found that  $c_Z^{-1}$  decreases monotonically with  $q$ . Thus the probability of detection will be maximized when  $q$  is minimized. Since  $q$  is invariant with an interchange of coefficients, the solutions  $c_i$  that minimize it all have the same value, say  $c$ . Substituting that symbol in (6.8) yields

$$\sqrt{WT} (1 - nc) = -\gamma \sqrt{1 + nc^2} \quad (6.11)$$

Squaring (6.11) yields a quadratic equation in  $c$ , and substituting the appropriate solution of that equation in (6.10) yields

$$q = \frac{\beta + \sqrt{n(n+1 - \beta^2)}}{n - \beta^2} \quad (6.12)$$

If

$$\frac{\beta}{\sqrt{n}} \equiv \frac{\gamma}{\sqrt{nWT}} < \frac{1}{10} \quad (6.13)$$

then

$$q \approx \sqrt{1 + n^{-1}} \quad (6.14)$$

It is clear from (6.9) that the signal-to-noise power ratio required to achieve a probability of detection of 0.5 is

$$r_T = \gamma q \div \sqrt{WT} \quad (6.15)$$

The quantity  $10 \log_{10} r_T$  is usually known as the recognition differential. It is clear from (6.14) that performance improves monotonically with  $n$ . However, the penalty associated with small  $n$  is not severe; for example, the degradation associated with  $n = 2$  is only 0.9 dB.

Figure 6.1 shows transition curves for cases in which the bandwidth is 600 Hz, the averaging time is five minutes, and the false alarm probability per channel is  $10^{-5}$ . The upper plot shows detection probability versus signal-to-noise power ratio for the case  $n = 2$  and the limiting case  $n \rightarrow \infty$ , which represents perfect estimation of background noise level. The spread of the curve for  $n = 2$  is noticeably greater than that for  $n \rightarrow \infty$ . (Spread is the value of  $r$  for  $P_D = 0.8$  less that for  $P_D = 0.2$ .) To a first level of approximation, spread is proportional to  $q$ . The lower plot shows detection probability for the same cases as a function of  $10 \log_{10} r$ . To a first level of approximation, the spread of these curves is independent of  $q$ .

## 6.2 Special Case: $P_i(t) = P_N$

This section extends the results of the previous section to apply to cases in which sonar detection experiments are conducted in randomly selected environments. The analysis



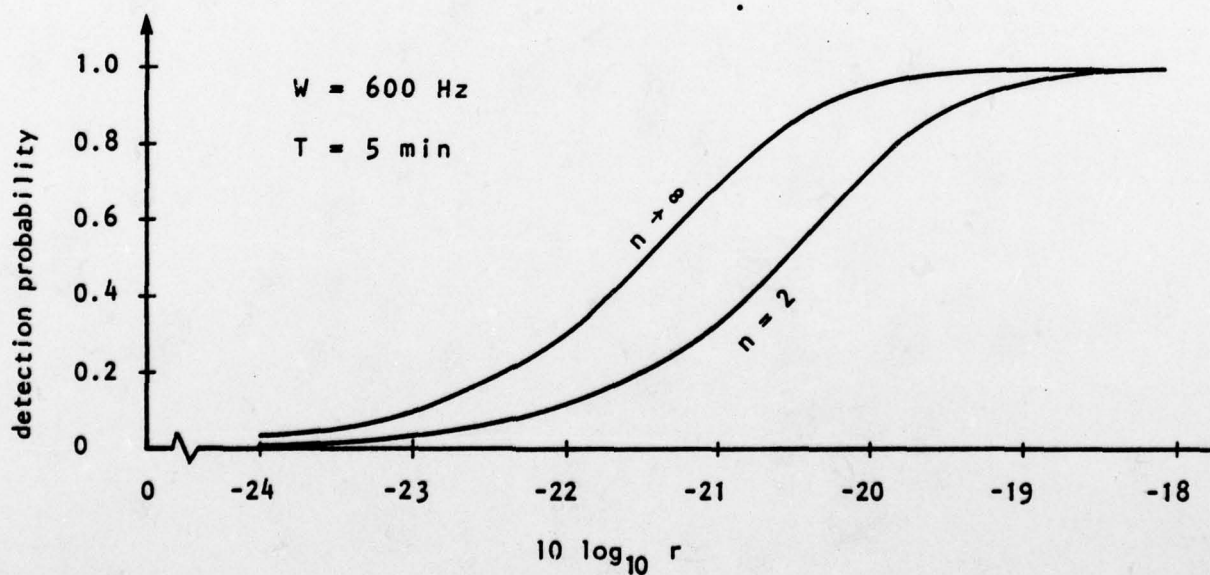
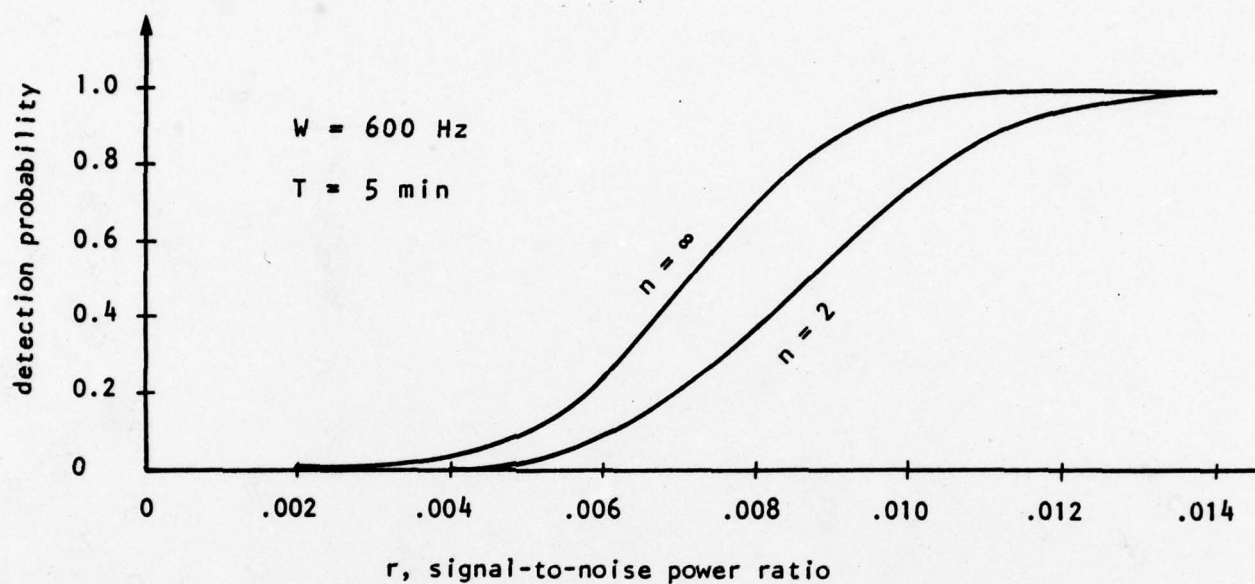


FIGURE 6.1 Transition Curves.

is based on a special case of the compound process in which

$$P_S(t) = P_S \quad (6.16)$$

$$P_i(t) = P_N, \quad i = 0, 1, 2, \dots, n \quad (6.17)$$

where  $P_S$  and  $P_N$  are statistically independent random variables. The signal and noise processes are thereby non-ergodic and non-Gaussian; however, they are conditionally Gaussian given  $P_S$  and  $P_N$ . The results also apply to cases in which the relaxation times of the power envelope processes are very long compared to the post-rectification averaging period.

The result (6.9) of the previous section is utilized to obtain the inverse of the conditional coefficient of variation of the test statistic:

$$\frac{1}{c_Z} = \frac{\sqrt{WT} R - \gamma q}{\sqrt{R^2 + 2R + q^2}} \quad (6.18)$$

where  $R = P_S \div P_N$ , a random variable, is the signal-to-noise-power ratio for a single experiment.

If the time-bandwidth product is adequate, the conditional distribution of the test statistic is approximately normal, and the conditional probability of detection can be expressed as

$$P(D|R) = N(1 \div c_Z) \quad (6.19)$$

where  $N( )$  is the probability distribution function for a zero-mean unit variance normal variate. The dependence of  $C_Z$  on  $R$  is given by (6.18). The probability of detection is

$$P_D = E[N(1/c_Z)]$$

$$= \int_0^{\infty} dr f_R(r) N \left[ \frac{\sqrt{WT} r - \gamma q}{\sqrt{r^2 + 2r + q^2}} \right] \quad (6.20)$$

where  $f_R( )$  is the probability density function for  $R$ , which can be calculated from\*

$$f_R(r) = \int_0^{\infty} ds s f_S(rs) f_N(s) \quad (6.21)$$

where  $f_S( )$  is the probability density function for  $P_S$  and  $f_N( )$  is the probability density function for  $P_N$ .

If the distribution of  $R$  is broad with respect to the width of the transition curve, then the latter can be approximated by a step function with the transition occurring at  $r_T$ , defined per (6.15), and the approximation of (6.20) is

$$P_A = \int_{r_T}^{\infty} dr f_R(r) \quad (6.22)$$

A quantity that is often employed in sonar analysis is

$$N_E = 10 \log_{10} (R \div r_T) \quad (6.23)$$

\*Ref. 5, page 197.



which is the so-called "signal excess", the signal-to-noise ratio in dB in excess of that required for a conditional probability of detection of 0.5. If the corresponding change of variables is made in (6.22), the result is

$$P_A = \int_0^{\infty} de f_E(e) \quad (6.24)$$

where  $f_E(e) = 0.23r_{TE}^{0.23e} f_R(r_{TE}^{0.23e})$  is the probability density function for the excess signal-to-noise ratio in dB. The form (6.24) is often employed with the assumption that  $E$  is normally distributed. Reference 14 compares the predictions made using that form with  $N_E$  normally distributed to those using the density function for a short-noise process.

The difference between the predictions of (6.20) and its approximation (6.22) will be shown by means of several examples. It is assumed that both signal and noise envelopes are gamma variables\* with respective densities

$$f_P(u) = \frac{a}{p_S \Gamma(a)} \left( \frac{a}{p_S} u \right)^{a-1} \exp \left( - \frac{a}{p_S} u \right), \quad u \geq 0 \quad (6.25)$$

$$g_P(u) = \frac{b}{p_N \Gamma(b)} \left( \frac{b}{p_N} u \right)^{b-1} \exp \left( - \frac{b}{p_N} u \right), \quad u \geq 0 \quad (6.26)$$

where  $p_S = E(P_S)$

$p_N = E(P_N)$

---

\*The utilization of the gamma density for the noise envelope is suggested in Reference 15.

The parameters  $a$  and  $b$  determine the respective coefficients of variation of the envelopes. For example, the coefficient of variation for the signal is  $1/\sqrt{a}$ .

Substituting (6.25) and (6.26) in (6.21) and evaluating the integral gives the density of the signal-to-noise power ratio:

$$f_R(r) = \frac{\Gamma(a+b)}{\Gamma(a)\Gamma(b)} \left( \frac{ap_N}{bp_S} \right)^a \frac{r^{a-1}}{\left( 1 + \frac{ap_N}{bp_S} r \right)^{a+b}} \quad (6.27)$$

The result is seen to be a generalization of the F density in which  $p_S \div p_N$  is a scale factor.\* The mode, mean, and variance of  $R$  are

$$\text{mode} = \frac{a-1}{a} \cdot \frac{b}{b+1} \cdot \frac{p_S}{p_N} \quad (6.28)$$

$$m_R = \frac{b}{b-1} \cdot \frac{p_S}{p_N}, \quad b > 1 \quad (6.29)$$

$$\sigma_R^2 = \frac{b+a-1}{a(b-2)} m_R^2, \quad b > 2 \quad (6.30)$$

---

\*The special case  $a = 1$  corresponds to a Rayleigh fading (narrow-band) signal. This case was discussed in a presentation at the 94th meeting of the Acoustical Society of America, December, 1977, by J. C. Heine and J. R. Nitsche.

Dividing (6.29) by the square root of (6.30) gives the coefficient of variation

$$c_R = \sqrt{\frac{b+a-1}{a(b-2)}}, \quad b > 2 \quad (6.31)$$

It is seen from (6.29) that  $m_R > p_S \div p_N$ ; that is,  $p_S \div p_N$  is not the mean signal-to-noise power ratio.

The probability of detection and its approximation will be calculated by substituting (6.27) in (6.20) and (6.22) respectively. The receiver parameters are those of one of the cases examined in Section 6.1 in which the bandwidth is 600 Hz, the averaging time is five minutes, the false alarm probability per channel is  $10^{-5}$ , and the noise background is estimated with two channels. Figures 6.2 through 6.7 show plots of  $P_D - P_A$  as a function of  $P_D$  for six pairs of values of the parameters  $a$  and  $b$ . Peak errors range from nearly 0.01 to 0.03. For detection probabilities greater than about 0.2, these errors are small. For smaller probabilities, the percentage of error increases.

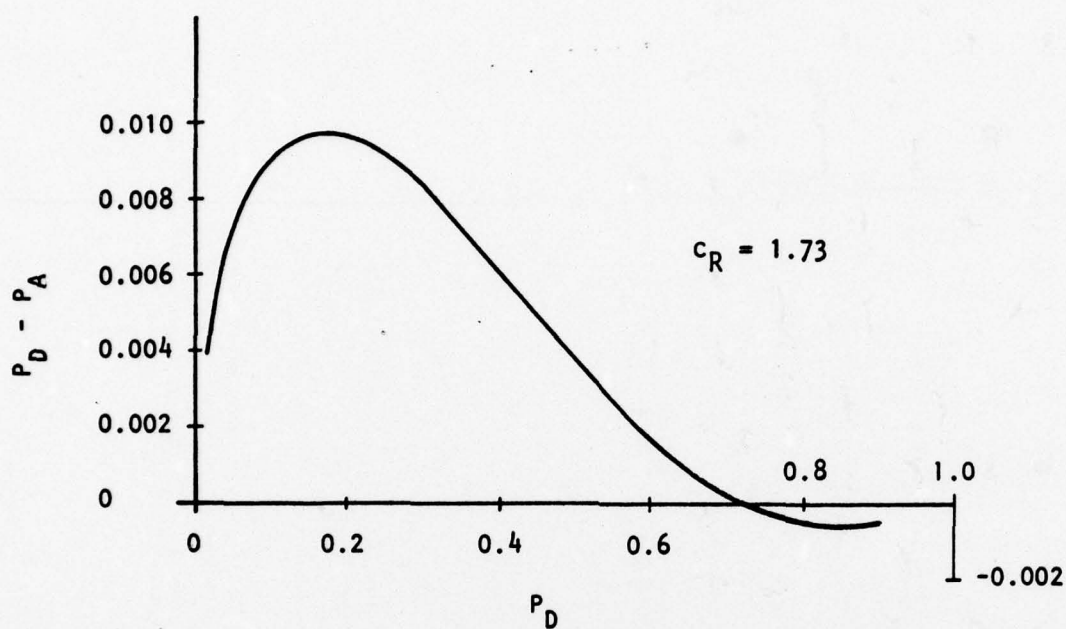
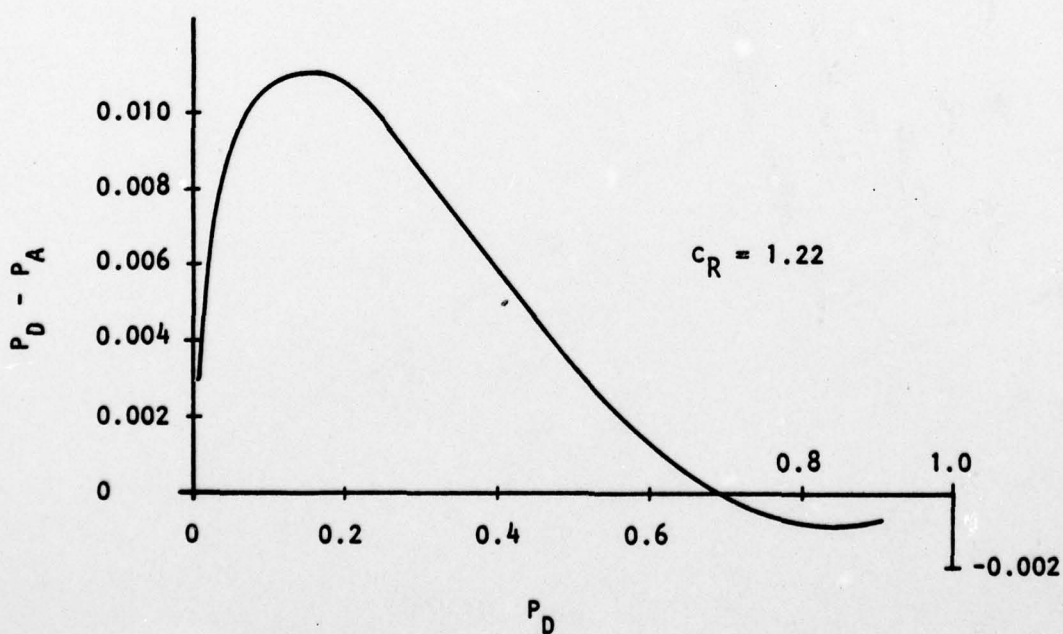
For integer values of the parameters  $a$  and  $b$  in the density function (6.27), the integral (6.22) can be expressed as a closed form. The forms given below are readily evaluated by means of a small digital calculator.

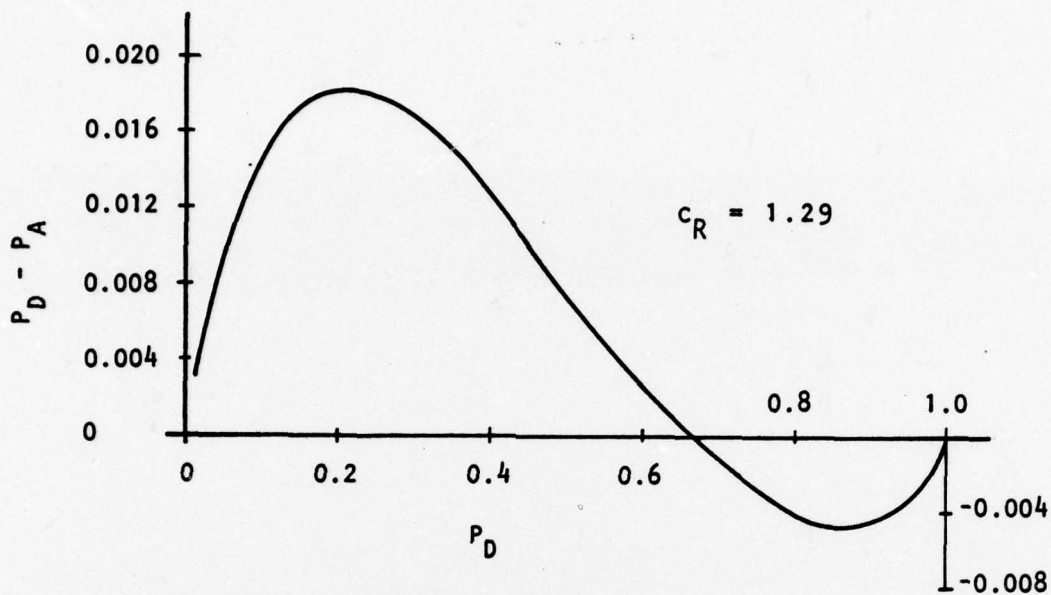
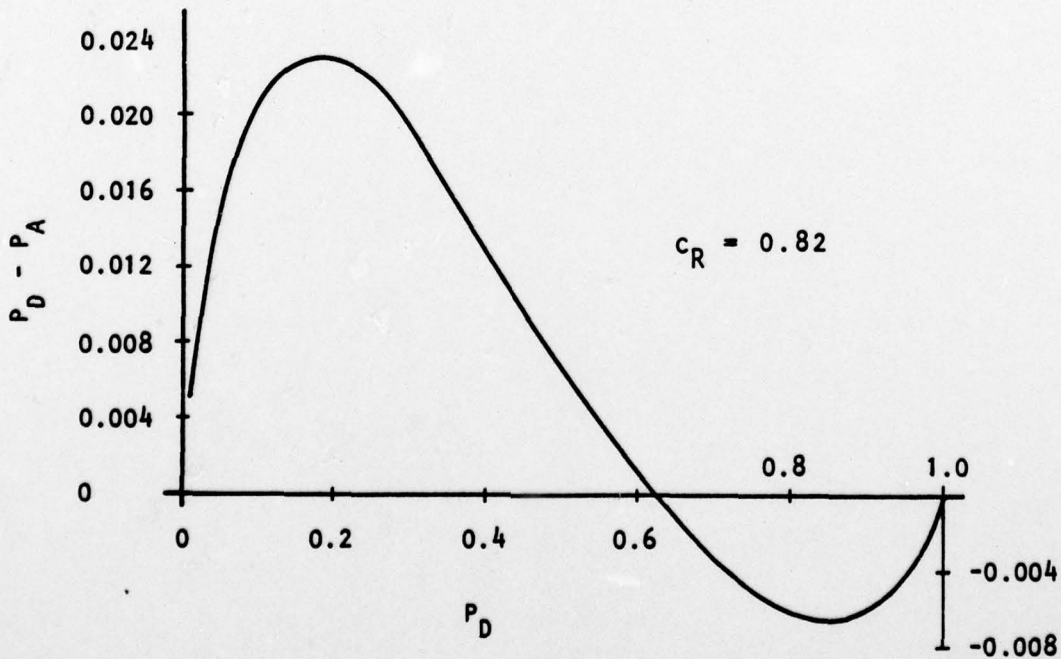
$$P_A = Q^b, \quad \text{for } a = 1 \quad (6.32)$$

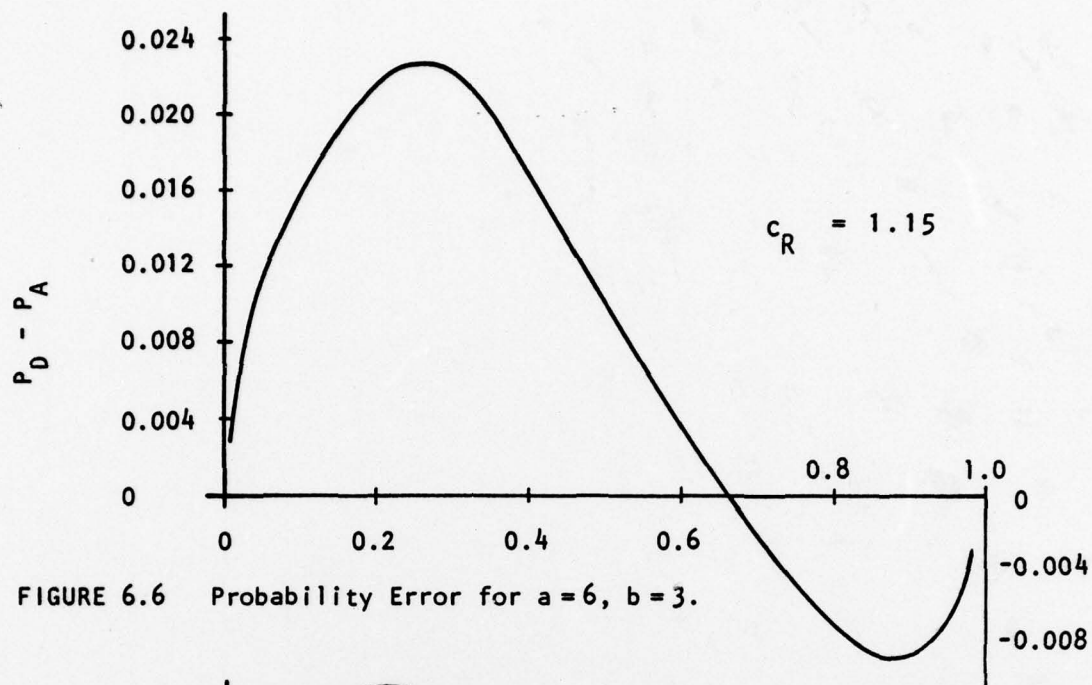
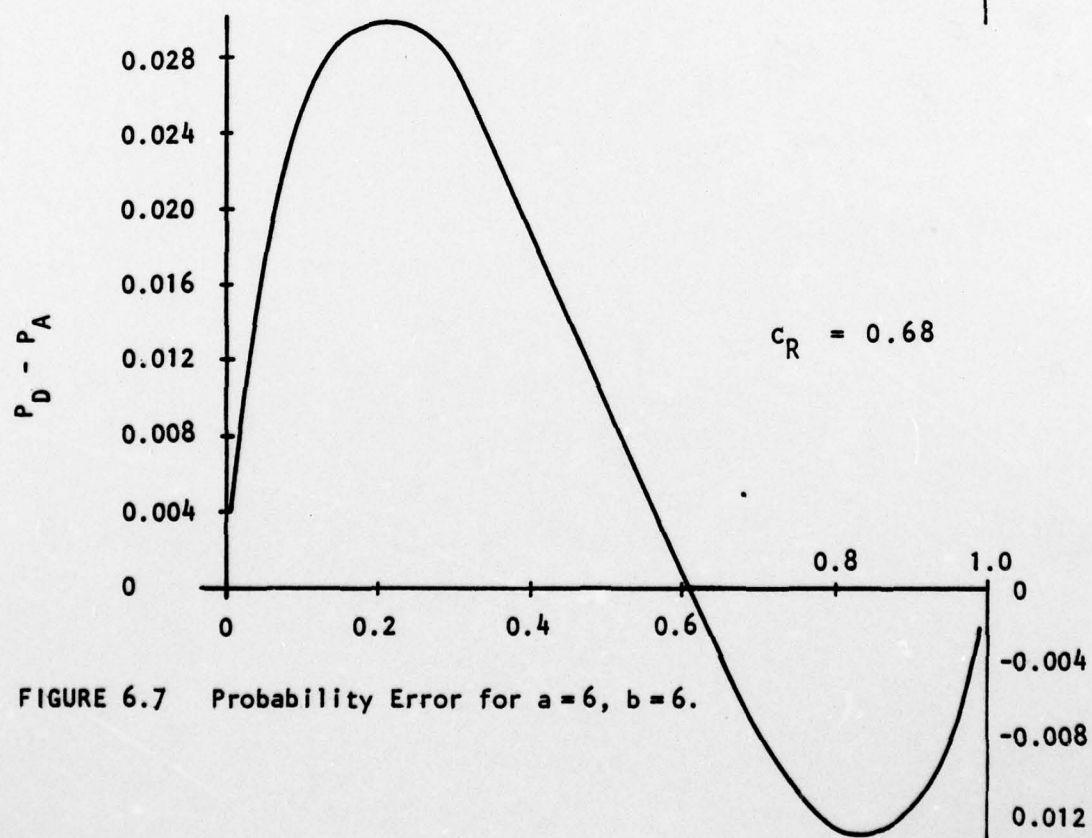
$$= Q^b(b + 1 - bQ), \quad \text{for } a = 2 \quad (6.33)$$

$$= \frac{1}{2} Q^b \left[ (b+2)(b+1) - 2(b+2)bQ + (b+1)bQ^2 \right], \quad \text{for } a = 3 \quad (6.34)$$



FIGURE 6.2 Probability Error for  $a = 1$ ,  $b = 3$ .FIGURE 6.3 Probability Error for  $a = 1$ ,  $b = 6$ .

FIGURE 6.4 Probability Error for  $a = 3$ ,  $b = 3$ .FIGURE 6.5 Probability Error for  $a = 3$ ,  $b = 6$ .

FIGURE 6.6 Probability Error for  $a=6$ ,  $b=3$ .FIGURE 6.7 Probability Error for  $a=6$ ,  $b=6$ .



$$\text{where } Q = \left( 1 + \frac{a r_T \div b}{p_S \div p_N} \right)^{-1}$$

b is an integer.

Transition curves for six cases are given in Figures 6.8 through 6.10, which also show the transition curve for a receiver with a two-channel threshold operating in Gaussian noise. It is seen that the spread is primarily determined by the parameter a. (The coefficient of variation of the signal power envelope is  $1 \div \sqrt{a}$ .) The case  $a = 1$  corresponds to a Rayleigh fading signal.

AD-A062 487 BOLT BERANEK AND NEWMAN INC ARLINGTON VA

F/G 17/1

CE IN ENVIRONMEN--ETC(U)

N00014-77-C-0303

NL

AD  
A082187

END  
DATE  
FILMED  
3-79  
DDC

3-79

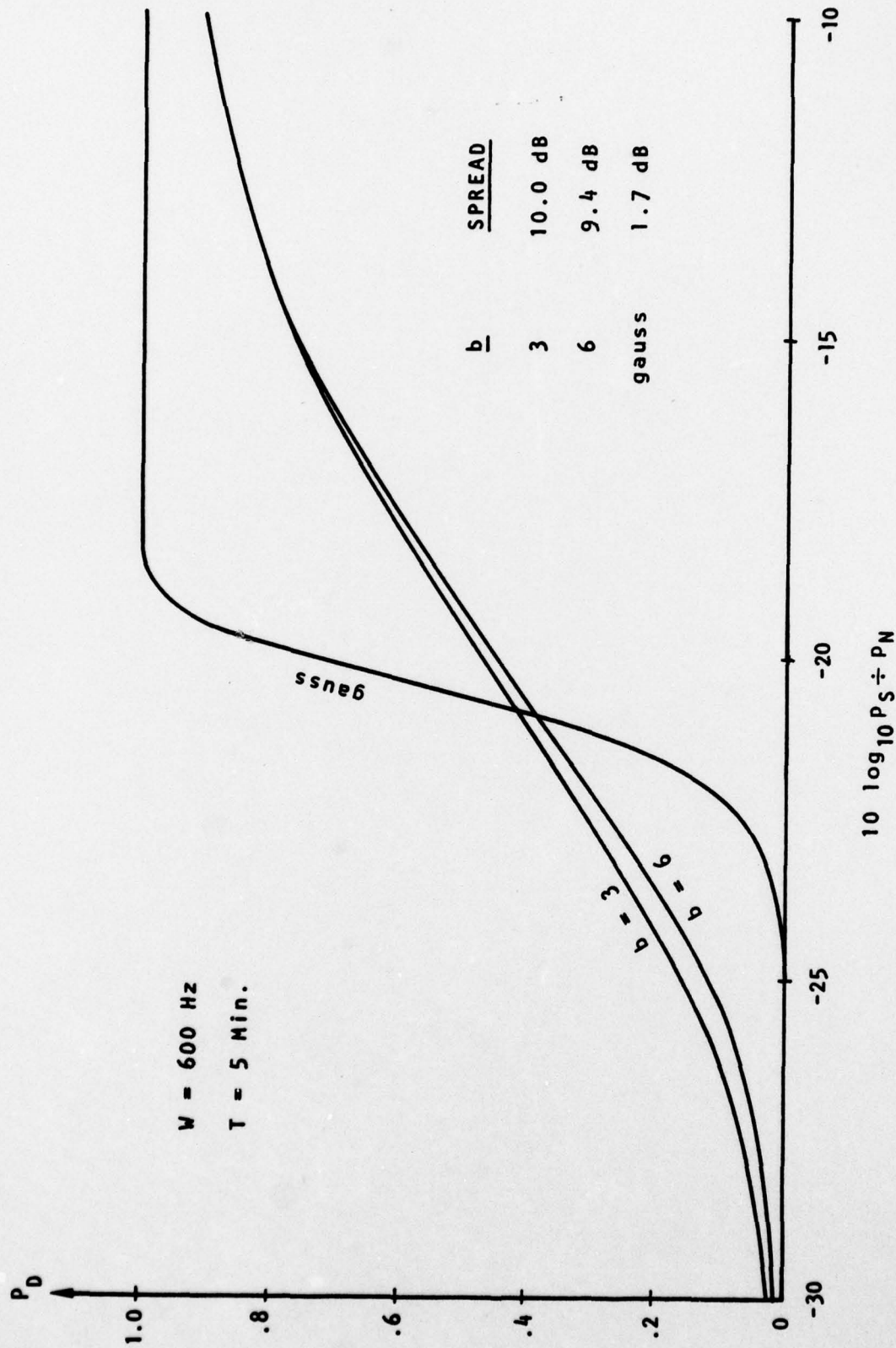


FIGURE 6.8 Transition Curves for  $a = 1$ .



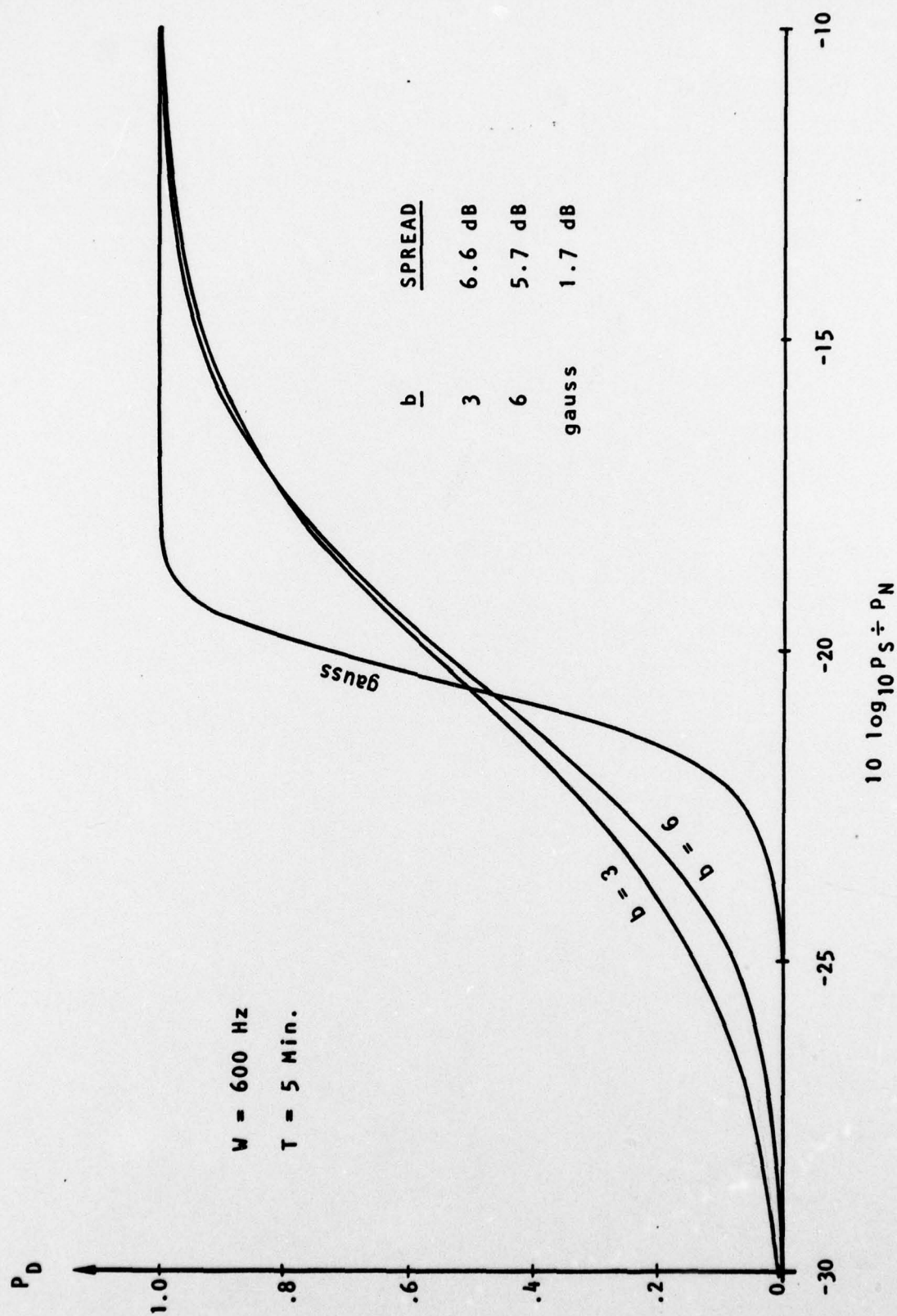


FIGURE 6.9 Transition Curves for  $a = 3$ .

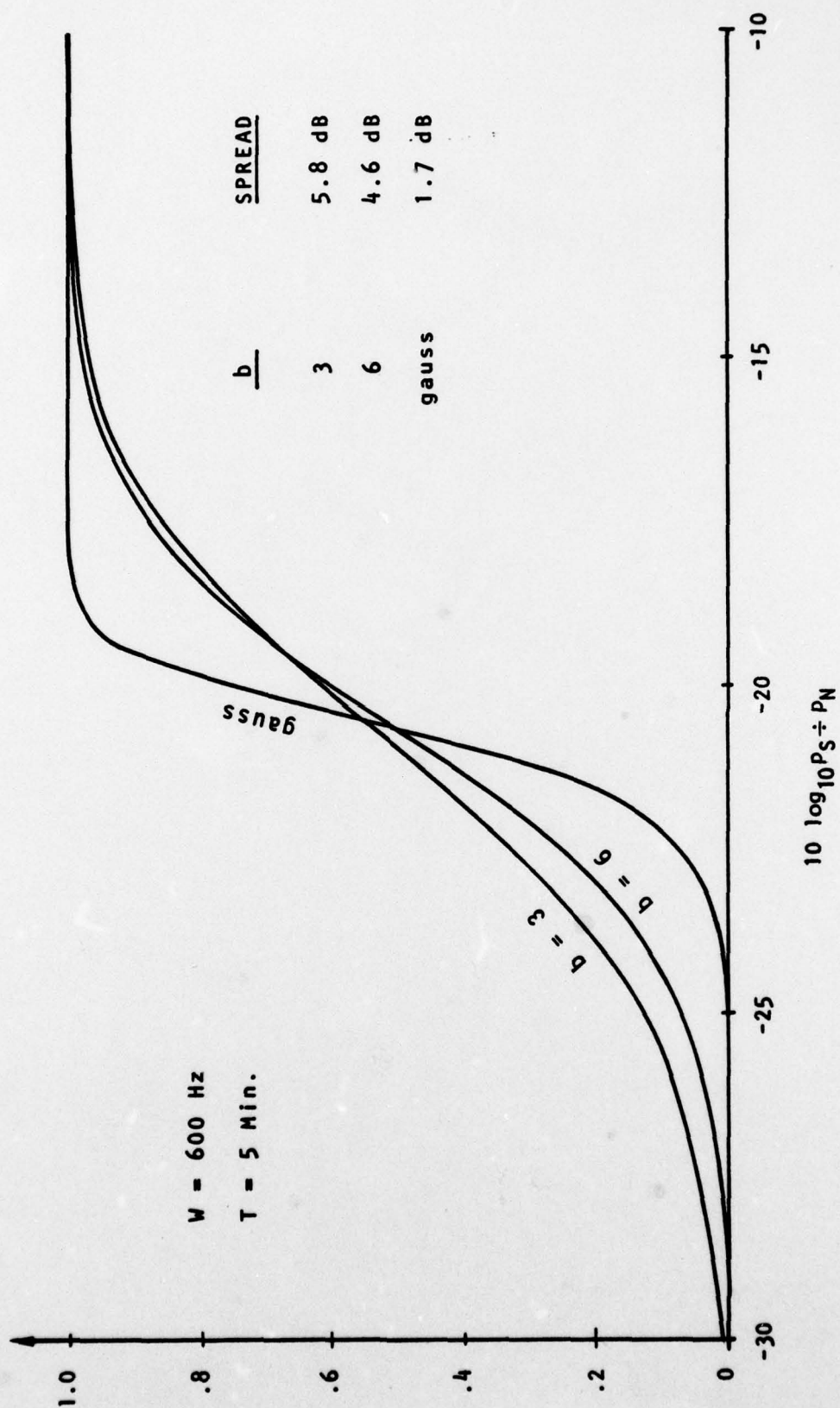


FIGURE 6.10 Transition Curves for  $a = 6$ .

7.0 SPECIAL CASE:  $P_i(t) = P_N(t)$ 

This section investigates the special case in which the noise processes have a common power envelope process: i.e.,  $P_1(t) = P_N(t)$ ,  $i = 0, 1, 2, \dots, n$ . This case is relevant to the case of a multi-beam system whose performance is limited by wave noise. Since noise level is related to average wind speed, and since average wind speed is correlated over a large area, it seems reasonable to expect the power envelopes of different channels to be highly correlated. A similar phenomenon might be expected with a frequency analyzer operating in a frequency band in which the ambient noise is dominated by shipping. Since all channels are viewing the same sources, it is reasonable to expect a high correlation of noise power envelope from bin to bin if the power spectra of the sources are reasonably smooth. The case to be examined is a limiting case in which the noise power envelopes are perfectly correlated.

Additional assumptions are listed below.

1. The noise power envelope process is given by (4.23).
2. The parameters of all channels are identical.
3. The signal is a stationary Gaussian process; therefore,  $P_S(t) = p_S$ , a constant.
4. The weighting coefficients  $c_i$  for threshold formation are those derived in Section 6.1.



5. The number of channels employed for threshold formation is large.
6. All spectral functions have the same rectangular passband of width W.

The initial objective of the analysis is to evaluate the first three moments of the test statistic for this case.

For the general case, the mean value of the test statistic is given by (5.3); for the case at hand, this may be expressed as

$$m_Z = p_S - p_N \sum_{i=0}^n c_i \quad (7.1)$$

Given Assumptions 4 and 5, the indicated sum of the weighting coefficients is  $\gamma \div \sqrt{WT}$ , where  $\gamma$  is a false alarm parameter, W is input bandwidth, and T is averaging time. Thus

$$m_Z = p_S - \frac{\gamma}{\sqrt{WT}} p_N \quad (7.2)$$

where  $p_N = E[P_N(t)]$

For the general case, the variance of the test statistic is given by (5.17); for the case at hand, this may be expressed as

$$\sigma_Z^2 = (WT)^{-1} \left[ p_S^2 + 2p_S p_N + \left( p_N^2 + \sigma_P^2 \right) \sum_{i=0}^n c_i^2 \right] + \left( \sum_{i=0}^n c_i \right)^2 \sigma_P^2 I_D \quad (7.3)$$

where  $I_D = T^{-1} \int_{-T}^T dy (1 - |y|T^{-1}) r^2(y)$

$\sigma_P^2$  is the variance of  $P_N(t)$ , the noise power envelope

$r(\ )$  is defined per (4.30) or (4.46)

Given Assumptions 4 and 5,  $\sum_{i=0}^n c_i^2 \approx 1$ ; thus, after the terms are regrouped, the result is

$$\sigma_Z^2 \approx (WT)^{-1} \left[ \left( p_S + p_N \right)^2 + \sigma_P^2 \left( 1 + \gamma^2 I_D \right) \right] \quad (7.4)$$

For the general case, the expression for the third central moment of the test statistic is given in Table 2, in Section 5.0. Applying all of the assumptions except 5 gives

$$\mu_{3Z} = (TW)^{-2} \left\{ 6p_N p_S^2 + 6p_S (p_N^2 + \sigma_P^2) + 2p_S^3 - 2 \left[ p_N^3 p_P + 3p_N \sigma_P^2 + p_N^3 \right] \sum_{i=0}^n c_i^3 \right\}$$

continued....

$$\begin{aligned}
& - 3WT \left[ 2 \left( \sum_{i=0}^n c_i \right) p_S \sigma_P^2 + \left( \sum_{i=0}^n \sum_{j=0}^n c_i^2 c_j \right) (p_N^3 \beta_P + 2p_N \sigma_P^2) \right] I_D \Bigg\} \\
& - p_N^3 \beta_P \left( \sum_{i=S}^n c_i \right)^3 I_T
\end{aligned} \tag{7.5}$$

where  $I_T = 6T^{-2} \int_0^T dx r(x) (1 - xT^{-1}) \int_0^x dy r(x-y)r(y)$

$\beta_P = 2^3 n^{-2}$  for the power envelope process defined by (4.23)

$= [2(1-a)]^3 \div (1-a^3)$  for the envelope process defined by (4.37)

With the application of Assumption 5, the sum  $\sum_{i=0}^n c_i^3$  is approximately minus one; thus

$$\begin{aligned}
\mu_{3Z} &= (TW)^{-2} \Bigg\{ 6 \left[ p_N p_S^2 + p_S (p_N^2 + \sigma_P^2) + p_N \sigma_P^2 \right] \\
&+ 2 \left[ p_S^3 + p_N (1 + \beta_P) \right] \\
&- 3\gamma \sqrt{WT} \left[ 2(p_S + p_N) \sigma_P^2 + p_N^3 \beta_P \right] I_D \\
&- \left( \gamma p_N \right)^3 \sqrt{WT} \beta_P I_T \Bigg\}
\end{aligned} \tag{7.6}$$



If the square root of the time-bandwidth product is very large, certain terms in the expressions for the variance and the third central moment of the test statistic may be neglected. The ratio of the mean of the test statistic to its standard deviation is then

$$m_Z \div \sigma_Z = \left( \frac{r}{r_T} - 1 \right) \frac{\gamma}{\sqrt{B}} \quad (7.7)$$

where  $r = p_S \div p_N$

$$r_T = \gamma \div \sqrt{WT}$$

$$B = 1 + c_P^2 (1 + \gamma^2 I_D)$$

$$c_P = p_N \div \sigma_P$$

The coefficient of skewness of the test statistic is then

$$\mu_{3Z} \div \sigma_Z^3 = -\gamma \left[ 3(\beta_P + 2c_P^2) I_D + \gamma^2 \beta_P I_T \right] B^{-3/2} \quad (7.8)$$

The integrals  $I_D$  and  $I_T$  have been evaluated for the case in which the autocovariance function for the power envelope is

$$K_P(u) = \sigma_P^2 \exp(-|t|D^{-1}) \quad (7.9)$$

where  $D$  is the relaxation time of the envelope process. For the power envelope processes described in Section 4.3,

$$K_P(u) = [\sigma_P r(u)]^2 \quad (7.10)$$

where  $r(\ )$  is the autocovariance function for the Gaussian processes whose squares are the components of the envelope process. Using (7.9) and (7.10) gives

$$r(u) = \exp[-|t|(2D)^{-1}] \quad (7.11)$$

Evaluating the integrals shown below (7.3) and (7.5) with this function gives

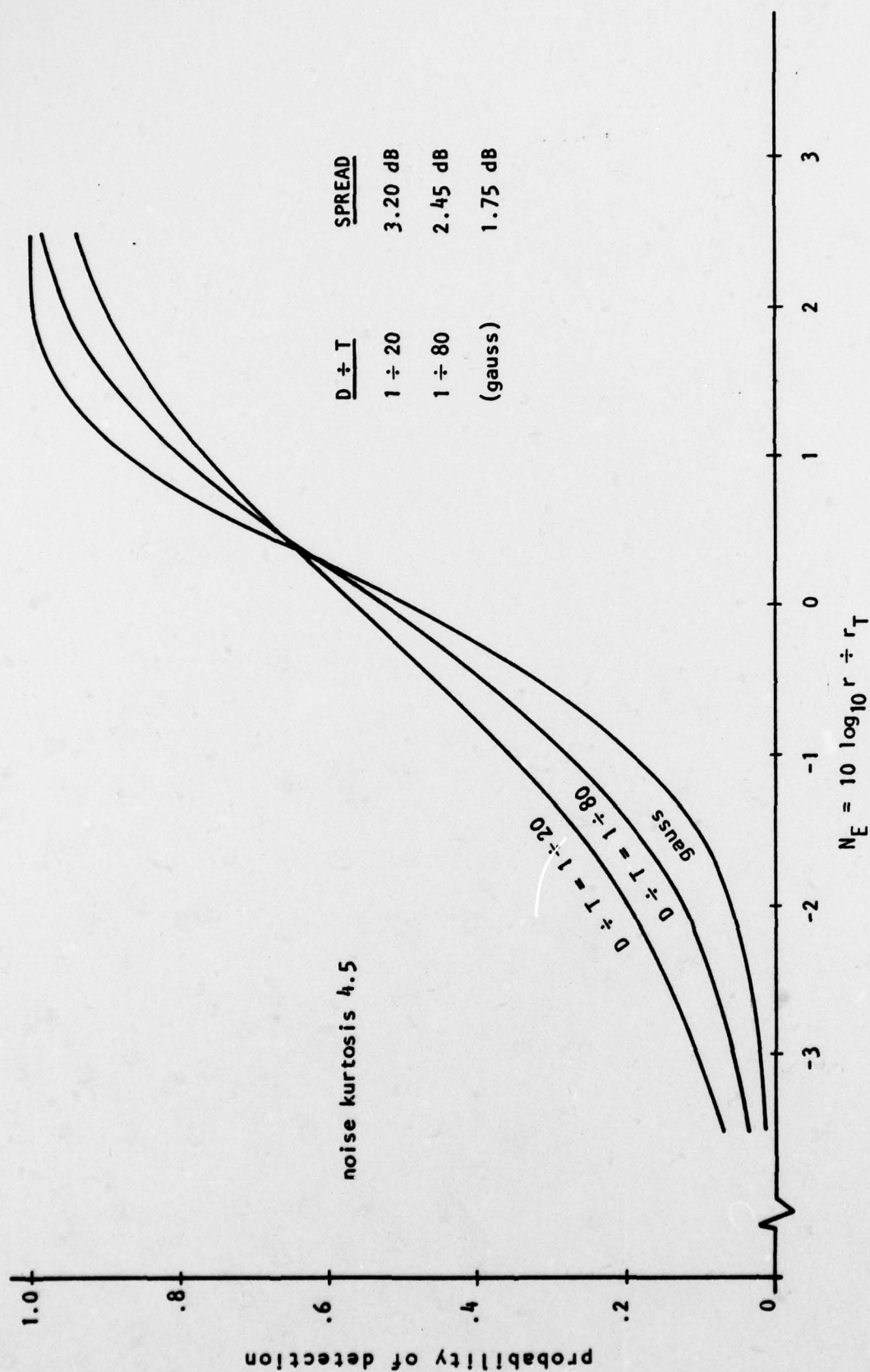
$$I_D = (4D \div T) [1 + (2D \div T) (\exp - T \div 2D - 1)] \quad (7.12)$$

$$I_T = 6(2D \div T)^2 [1 - 4D \div T + (1 + 4D \div T) \exp - T \div 2D] \quad (7.13)$$

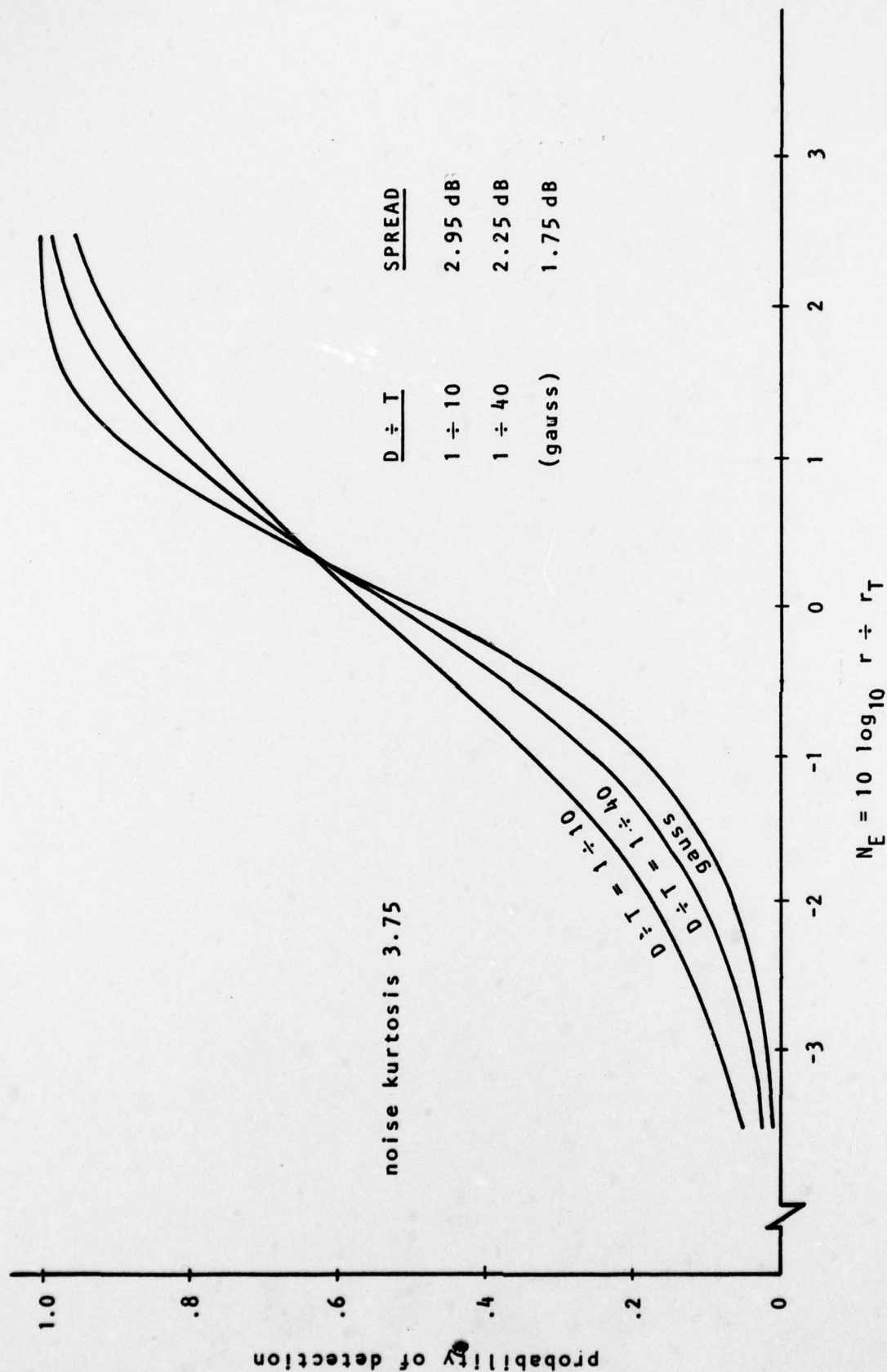
The results given above will first be applied to cases in which the distribution of the test statistic deviates moderately from normal, and (3.11) can be used to compute the probability of detection. The noise envelope process is assumed to be a normalized chi-square (NCS) process. Figure 7.1 shows transition curves for cases in which the NCS process has four degrees of freedom, yielding a kurtosis of 4.5 for the input noise process.\* It is seen that the spread of the transition curves increases with the ratio  $D/T$  of the envelope relaxation time to the receiver averaging time. The transition curve pertaining to Gaussian noise is also shown. Figure 7.2 shows transition curves for cases in which the NCS process has eight degrees of freedom, yielding a kurtosis of 3.75 for the input noise process.

---

\*For a Gaussian process, the kurtosis is 3.0.

FIGURE 7.1 Transition Curves for NSC Envelope,  $n = 4$ .



FIGURE 7.2 Transition Curves for NSC Envelope,  $n = 8$ .

Both figures show that small values of  $D/T$  produce significant spreading of the transition curves.

For larger values of  $D/T$ , the distribution of the test statistic will be considerably non-normal, and (3.11) cannot be used to predict the probability of detection. In order to proceed further, an alternative to the normal density is required for a basis function in (3.4). A density function for the test statistic will be derived for the limiting case described in Section 6.2, in which  $P_1(t) = P_N$ ; that is, the noise envelope is a time-invariant random variable.

In the case discussed above, the multichannel input noise processes are given by

$$N_1(t) = \sqrt{P_N} G_1(t) \quad (7.14)$$

For the case of noise alone, substituting (7.14) in (2.9) gives

$$Z = -P_N \sum_{i=0}^n c_i T^{-1} \int_0^T du G_1^2(u) \quad (7.15)$$

This result can be expressed as the product of two independent random variables:

$$B = PW \quad (7.16)$$

where  $B \equiv Z$  for this special case

$$P \equiv P_N$$

$$W = - \sum_{i=0}^n c_i T^{-1} \int_0^T du G_1^2(u) \quad (7.17)$$

If the bandwidths of the independent normal processes  $G_1(t)$  are very large compared to the reciprocal of the post-rectification averaging time  $T$ , then the variates represented by the integrals in (7.17) are nearly normal; furthermore, a linear combination of these variates is even more nearly normal. Thus, in most cases of interest, the random variable  $W$  can be considered as normal, and the density of  $B$  can be obtained if the density of  $P$  is specified.

One form for the density function of  $B$  is

$$f_B(x) = \int_0^{\infty} dy f_P(y) f_W(xy^{-1}) y^{-1} \quad (7.18)$$

where  $f_P(\ )$  is the density function for  $P$ ; it is zero for negative values of its argument

$f_W(\ )$  is the density function for  $W$ .

An alternative form is

$$f_B(x) = \int_0^{\infty} dy f_P(xy^{-1}) f_W(y) y^{-1}, \quad x \geq 0 \quad (7.19)$$

$$= - \int_{-\infty}^0 dy f_P(xy^{-1}) f_W(y) y^{-1}, \quad x < 0 \quad (7.20)$$

The use of the results of Section 3.0 requires a basis function for a standardized random variable

$$U = \frac{B - m_B}{\sigma_B}, \quad (7.21)$$



and the density for this variable is

$$f_U(x) = \sigma_B f_B(\sigma_B x + m_B) \quad (7.22)$$

Substituting this result in (3.8), and that result in turn in (2.12) gives the probability that the test statistic exceeds the threshold value (zero):

$$P_E = I_0 + (\alpha_3 - m_3) A^{-1} \sum_{i=0}^3 \delta_i I_i \quad (7.23)$$

$$\text{where } I_1 = \sigma_B \int_{-m_Z/\sigma_Z}^{\infty} dx f_B(\sigma_B x + m_B) x^1$$

Let  $u = \sigma_B x + m_B$ ; then

$$I_1 = \int_L^{\infty} du f_B(u) \left( \frac{u - m_B}{\sigma_B} \right)^1 \quad (7.24)$$

$$\text{where } L = \sigma_B \left( \frac{m_B}{\sigma_B} - \frac{m_Z}{\sigma_Z} \right)$$

Substituting (7.19) and (7.20) in (7.23) gives

$$I_1 = A_1 + B_1, \quad L \leq 0 \quad (7.25)$$

$$\text{where } A_1 = \int_0^{\infty} dy f_W(y) y^{-1} \int_0^{\infty} du f_P(uy^{-1}) \left( \frac{u - m_B}{\sigma_B} \right)^1 \quad (7.26)$$

$$B_1 = - \int_{-\infty}^0 dy f_W(y) y^{-1} \int_L^0 du f_P(uy^{-1}) \left( \frac{u - m_B}{\sigma_B} \right)^1 \quad (7.27)$$

In the inner integrals, let  $v = uy^{-1}$ ; then

$$A_1 = \left( \frac{-m_B}{\sigma_B} \right)^1 \int_0^{\infty} dy f_W(y) \int_0^{\infty} dv f_P(v) \left( 1 - v y m_B^{-1} \right)^1 \quad (7.28)$$

$$B_1 = \left( \frac{-m_B}{\sigma_B} \right)^1 \int_{-\infty}^0 dy f_W(y) \int_0^{Ly^{-1}} dv f_P(v) \left( 1 - v y m_B^{-1} \right)^1 \quad (7.29)$$

In the integrands, the polynomials can be represented as sums:

$$A_1 = \left( \frac{-m_B}{\sigma_B} \right)^1 \sum_{j=0}^1 \binom{1}{j} C_j \quad (7.30)$$

$$B_1 = \left( \frac{-m_B}{\sigma_B} \right)^1 \sum_{j=0}^1 \binom{1}{j} D_j \quad (7.31)$$

$$\text{where } C_j = \left( -m_B \right)^{-j} \int_0^{\infty} dy f_W(y) y^j \int_0^{\infty} dv f_P(v) v^j \quad (7.32)$$

$$D_j = \left( -m_B \right)^{-j} \int_{-\infty}^0 dy f_W(y) y^j \int_0^{Ly^{-1}} dv f_P(v) v^j \quad (7.33)$$

$\binom{1}{j}$  is the binomial coefficient

In (7.32), the inner integral gives the moments of the random variable P; thus

$$C_j = \left( -m_B \right)^{-j} m_{jP} \int_0^{\infty} dy f_W(y) y^j \quad (7.34)$$

If the random variable  $W$  is assumed to be normal, then

$$f_W(y) = \frac{1}{\sigma_W \sqrt{2\pi}} \exp -1/2 \left( \frac{y-m_W}{\sigma_W} \right)^2 \quad (7.35)$$

If (7.35) is substituted in (7.34), and if the variable of integration is changed to  $x = (y-m_W) \div \sigma_W$  then

$$C_j = (-p_N)^{-j} m_{jP} \frac{1}{\sqrt{2\pi}} \int_{\gamma}^{\infty} dx (1 - x\gamma^{-1})^j \exp -x^2/2 \quad (7.36)$$

since  $m_B = p_N m_W$ . If the polynomial in the integrand is represented as a sum, and if the order of integration and summation are interchanged, then

$$C_j = (-p_N)^{-j} m_{jP} \sum_{k=0}^j \binom{j}{k} (-\gamma)^{-k} E_k \quad (7.37)$$

$$\text{where } E_k = \frac{1}{\sqrt{2\pi}} \int_{\gamma}^{\infty} dx x^j \exp -x^2/2 \quad (7.38)$$

$$E_0 = \frac{1}{\sqrt{2\pi}} \int_{\gamma}^{\infty} dx \exp -x^2/2 \equiv Q(\gamma) \quad (7.39)$$

$$E_1 = \frac{1}{\sqrt{2\pi}} \int_{\gamma}^{\infty} dx x \exp -x^2/2 \equiv n(\gamma) \quad (7.40)$$

$$E_2 = \gamma n(\gamma) + Q(\gamma) \quad (7.41)$$

$$E_3 = (2 + \gamma) n(\gamma) \quad (7.42)$$



If (7.39) through (7.42) are substituted as required in (7.37), and if the results are substituted as required in (7.30), the end results are

$$A_0 = Q(\gamma) \quad (7.43)$$

$$A_1 = p_N \sigma_W \sigma_B^{-1} n(\gamma) \quad (7.44)$$

$$A_2 = \left( p_N \sigma_W \sigma_B^{-1} \right)^2 \left\{ \left( 1 - c_P^2 \right) \gamma n(\gamma) + \left[ 1 + c_P^2 (1 + \gamma^2) \right] Q(\gamma) \right\} \quad (7.45)$$

$$A_3 = \left( p_N \sigma_W \sigma_B^{-1} \right)^3 \left\{ \left[ 6c_P^2 + (2 + \gamma^2) \left( 1 + \mu_{3P} \div p_N^3 \right) \right] n(\gamma) - \left[ 6c_P^2 + (3 + \gamma^2) \mu_{3P} \div p_N^3 \right] \gamma Q(\gamma) \right\} \quad (7.46)$$

To evaluate (7.33), assume that  $P_N$  is a gamma variable. Substituting (6.26) in (7.33) gives

$$D_j = \left( -m_B \right)^{-j} \int_{-\infty}^0 dy f_W(y) y^j \frac{b}{p_N \Gamma(b)} \int_0^{Ly^{-1}} dv \left( \frac{bv}{p_N} \right)^{b-1} \exp \left( - \frac{bv}{p_N} \right) v^j \quad (7.47)$$

Now let  $x = bvp_N^{-1}$ ; then

$$D_j = \left( \frac{p_N}{-m_B b} \right)^j \int_{-\infty}^0 dy f_W(y) y^j \Gamma^{-1}(b) \int_0^{bL(p_N y)^{-1}} dx x^{b+j-1} e^{-x} \quad (7.48)$$

The inner integral is evaluated by means of 3.381 No. 1. of Reference 13:

$$D_j = \left( \frac{p_N}{-m_B b} \right)^j \int_{-\infty}^0 dy f_W(y) y^j \gamma \left[ b+j, bL(p_N y)^{-1} \right] \Gamma^{-1}(b) \quad (7.49)$$

where  $\gamma( , )$  is the incomplete gamma function. If the random variable  $W$  is assumed to be normal, and if (7.35) is substituted in (7.49), and if the variable of integration is changed to  $x = -y(\gamma\sigma_W)^{-1}$  the result is

$$D_j = \gamma \frac{(-b)^{-j}}{\sqrt{2\pi}} \int_0^{\infty} dx x^j \exp \left[ -\frac{1}{2} (1-x)^2 \right] \gamma(b+j, bKx^{-1}) \Gamma^{-1}(b) \quad (7.50)$$

$$\text{where } K = -L(p_N \gamma \sigma_W)^{-1} \quad (7.51)$$

If the quantity  $L$ , defined below (7.24), is substituted in (7.51), the result obtained after algebraic operations is

$$K = \left( 1 - \frac{\sigma_B}{\sigma_Z} \cdot \frac{m_Z}{m_B} \right) \quad (7.52)$$

Then, utilizing (7.2) and (7.4) and simplifying the result gives

$$K = 1 + \sqrt{\frac{(r+1)^2 + c_P^2(1+\gamma^2)}{(r+1)^2 + c_P^2(1+\gamma^2 I_D)}} \left( \frac{r}{r_T} - 1 \right) \quad (7.53)$$

For the small-signal case ( $r \equiv p_S \div p_N < 1$ ), the parameter  $K$  depends primarily on the ratio of  $r$  to  $r_T$ .

If the noise distribution parameter  $b$  is an integer  $n$ , then, by 8.352 No. 1 of Reference 13,

$$\frac{\gamma(b+j, bKx^{-1})}{\Gamma(b)} = \frac{(b+j-1)!}{(n-1)!} \left[ 1 - \left( \sum_{m=0}^{b+j-1} \frac{(nKx^{-1})^m}{m!} \right) \exp -bKx^{-1} \right] \quad (7.54)$$

The coefficients  $\delta_1 A^{-1}$  required for (7.22) are derived from the moments of the standardized random variable  $U$  given by (7.21) using the determinants defined under (3.8). These moments are derived from the moments of the zero-mean random variable

$$\begin{aligned} V &= B - m_B \\ &= PW - p_N m_W \\ &= -p_N m_W \left[ 1 - p_N^{-1} (1 - GY^{-1}) \right] \end{aligned} \quad (7.55)$$

where  $G$  is a standardized normal random variable. The moments of  $V$  are given by



$$E[V^n] = (-p_N m_W)^n \sum_{i=0}^n \binom{n}{i} m_{1P} (-p_N)^{-1} \sum_{j=0}^1 \binom{1}{j} m_{1G} (-\gamma)^{-j} \quad (7.56)$$

If P is a gamma random variable,

$$m_{1P} p_N^{-1} = \frac{(b+1-1)!}{(b-1)! b^1} \quad (7.57)$$

and the moments of G are

$$m_{21G} = \frac{(21)!}{1! 2^1}$$

$$m(21+1)G = 0 \quad (7.58)$$

Values for plotting transition curves were calculated using (7.23) in which the value of the determinant A and values of  $\delta_1$  were obtained from the determinants given below (3.8). The required moments were calculated from (7.56) using (7.57) and (7.58). The normalized moment  $\alpha = \mu_{3Z} \div \sigma_Z^3$  was obtained from (7.8). The integrals  $I_1$  given by (7.25) were evaluated using (7.43) through (7.46) and (7.51). The latter were executed by means of a digital computer.

The transition curves are shown in Figure 7.3 for the cases in which the power envelope is a normalized chi-square with four degrees of freedom. The case  $T + D = 0$  is that in which the envelope is a random variable; i.e., time invariant.

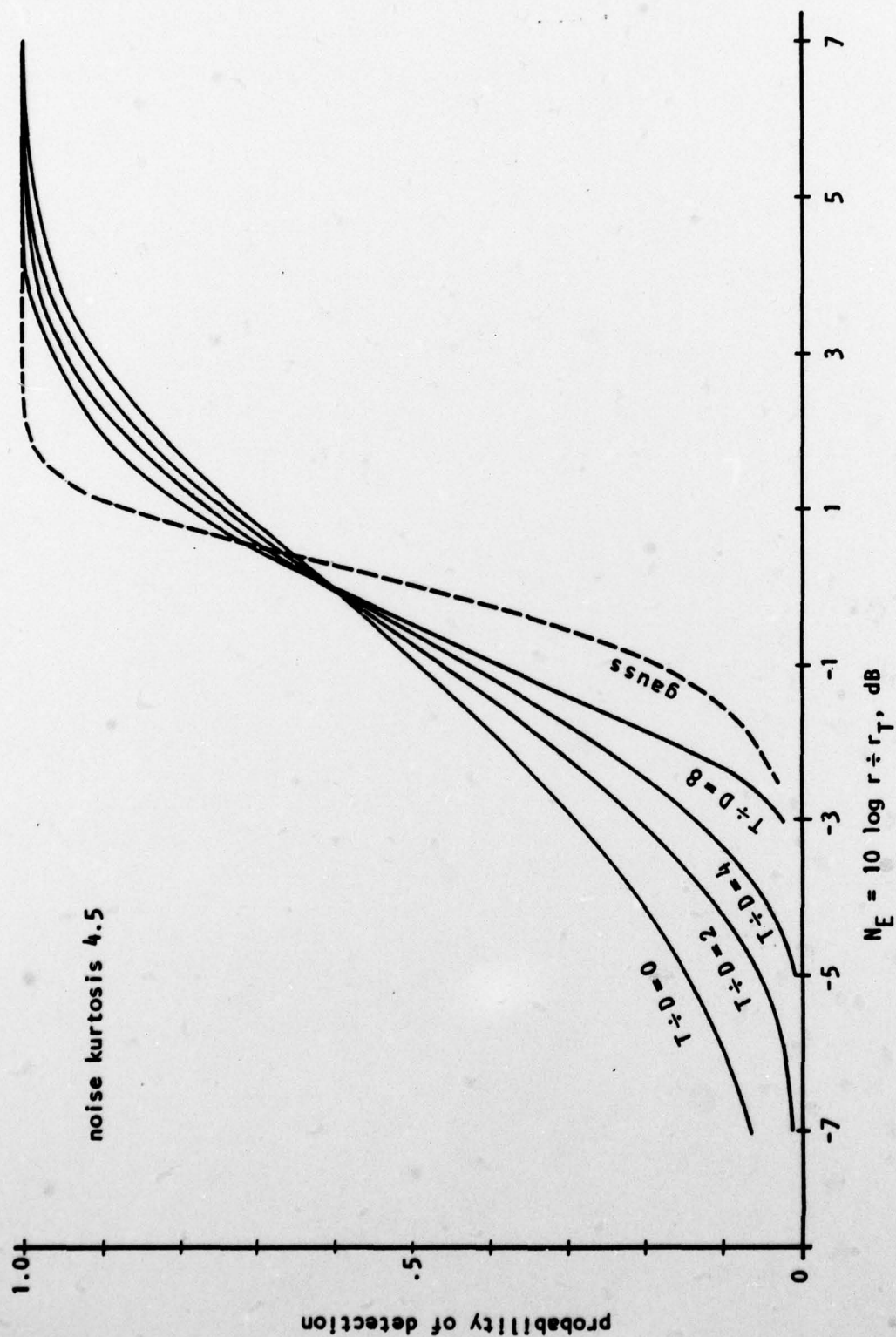


FIGURE 7.3 Transition Curves from Non-normal Basis.

References

1. M. Moll, R. Spooner, F. Jackson, "A Physical Approach to Dynamic Modeling of Detection Performance Using Preformed Beams in a Multiple Target Environment," Bolt Beranek and Newman Inc. Report No. 1634, 1 May 1972, AD 905-4116.
2. H. Cox, "Performance Prediction for Passive Sonar (U)," U. S. Navy Journal of Underwater Acoustics, Vol. 21, No. 3, July, 1971, pp. 461-472 (CONFIDENTIAL).
3. M. Moll, "Analytical Evaluation of the Effects of Variability on Passive Sonar Detection Performance," Proceedings of the First Workshop on Operations Research Models on Fluctuations Affecting Passive Sonar Detection (U)," Naval Ship Research and Development Center Report No. 76-0063 (Vol. I), pp. 133-161.
4. M. Moll, "Detection Performance of an Operator Using Lofar," Bolt Beranek and Newman Inc. Report No. 3225, April 1976.
5. A. Papoulis, "Probability, Random Variables, and Stochastic Processes," McGraw-Hill, New, York, New, York, 1965.
6. H. Cramér, "Mathematical Methods of Statistics," Princeton University Press, Princeton, N.J., 1946.
7. J. B. Farison, "On Calculating Moments of Some Common Probability Laws," IEEE Transactions on Information Theory, Vol. 1T-11, No. 4, October, 1965, pp. 586-9.
8. T. Arase and E. M. Arase, "Deep-Sea Ambient Noise Statistics," JASA, vol. 44, No. 6, 1968, pp. 1679-1684.
9. W. J. Jobst and S. L. Adams, "Statistical Analysis of Ambient Noise," JASA, Vol 62, No. 1, July, 1977, pp. 63-71.
10. M. Moll, "Analytical Evaluation of the Effects of Variability on Passive Sonar Detection Performance," Proceedings of the First Workshop on Operations Research Models Affecting Passive Sonar Detection (U)," NSRDC/C Report No. 76-0063, Vo. 1, January, 1976, (CONFIDENTIAL).



11. G. L. Wise and N. C. Gallagher, Jr., "On Spherically Invariant Random Processes," IEEE Trans. on Information Theory, Vol. IT-24, No. 1, January, 1978 (Correspondence).
12. D. Middleton, "An Introduction to Statistical Communication Theory," McGraw-Hill Book Co., Inc., New, York, New York, 1960.
13. I. S. Gradshteyn and I. M. Ryzhik, "Tables of Integrals, Series, and Products," Academic Press, New York, New York, 1965.
14. J. Goldman, "A Model of Broadband Ambient Noise Fluctuations due to Shipping (U)," Bell Laboratories OSTP-31JG, September, 1974, (CONFIDENTIAL).
15. J. C. Heine, "Recommendations for Modified Statistical Analysis of Ambient Noise Data," Bolt Beranek and Newman Inc. Technical Memorandum No. 385, November, 1977.
16. A. D. Whalen, "Effects of Fading Signals on Post-Detection Integration Receivers," Ref. 71 (Unclassified), June, 1967, in 21st Project Jezebel Interim Report (Secret).

AppendixAn Alternative Approach

An alternative approach to that discussed in Section 3.0 for predicting detection performance is based on the assumption that the averager outputs, and hence the test statistic, are conditionally normal\* given the power envelope functions.

The probability of the test statistic exceeding zero is given by (2.12) in terms of the density of the standardized test statistic  $Q$ . In analogous fashion, the conditional probability can be expressed as

$$P(Z \geq 0 | \underline{P}) = \int_{-m_{ZC} / \sigma_{ZC}}^{\infty} dq f_Q(q | \underline{P}) \quad (A-1)$$

where  $\underline{P} = \{P_i(t)\}$ ,  $i = S, 0, 1, 2, \dots, n$

$m_{ZC}$  is  $E(Z | \underline{P})$

$\sigma_{ZC}^2$  is  $\text{Var}(Z | \underline{P})$

If  $Z$  is conditionally normal, then

$$P(Z \geq 0 | \underline{P}) = N(m_{ZC} / \sigma_{ZC}) \quad (A-2)$$

where  $N(\ )$  is the normal distribution function for a variate with zero mean and unit variance

---

\*An approach based on conditional normality was described in Reference 16 and applied to a case with a Rayleigh Fading signal and normal noise.

An expression for the test statistic is given by (5.1). If the inputs to the multichannel analog are processes of the type given by (4.5), the test statistic is then

$$Z = 2T^{-1} \int_0^T du \sqrt{P_S(u)P_0(u)} G_S(u)G_0(u) - \sum_{i=S}^n c_i T^{-1} \int_0^T du P_i(u)G_i^2(u) \quad (A-3)$$

The mean value of  $Z$  conditioned on the power envelope functions is

$$E(Z|\underline{P}) = - \sum_{i=S}^n c_i A_i \quad (A-4)$$

where  $A_i = T^{-1} \int_0^T du P_i(u)$  is a random variable that is a finite time average of the  $i$ th power envelope.

The conditional variance of the test statistic is the conditional expected square less the conditional mean squared; the result is

$$\begin{aligned} \text{Var}(Z|\underline{P}) = & 4T^{-2} \int_0^T du \int_0^T dv \sqrt{M_S(u)M_S(v)M_0(u)M_0(v)\rho_S(u-v)\rho_0(u-v)} \\ & + \sum_{i=S}^n c_i^2 2T^{-2} \int_0^T du \int_0^T dv M_i(u)M_i(v)\rho_i^2(u-v) \end{aligned} \quad (A-5)$$

where  $\rho_i(\ )$  is the autocovariance of  $G_i(t)$ .



Convenient approximations for the terms of (A-5) will be derived. With a change of variables  $x = u+v$  and  $y = u-v$ , the ith integral of the second term is

$$I_1 = T^{-2} \int_{-T}^0 dy \rho_1^2(y) \int_{-y}^{y+2T} dx P_1[\frac{1}{2}(x+y)] P_1[\frac{1}{2}(x-y)] \\ + T^{-2} \int_0^T dy \rho_1^2(y) \int_y^{-y+2T} dx P_1[\frac{1}{2}(x+y)] P_1[\frac{1}{2}(x-y)] \quad (A-6)$$

If the correlation time of the process  $G_1(t)$  is much shorter than the correlation time of the power envelope process, the contributions of the inner integrals are significant only in a small region around  $y = 0$ ; thus

$$I_1 \approx T^{-2} \int_{-T}^T dy \rho_1^2(y) \int_0^{2T} dx M_1^2(x/2) \quad (A-7)$$

If the correlation time of  $G_1(t)$  is much shorter than  $T$ , and if the variable of integration of the second integral is changed to  $u = x/2$ , then

$$I_1 = T^{-1} W_1^{-1} B_1 \quad (A-8)$$

where  $W_1^{-1} = 2 \int_{-\infty}^{\infty} dy \rho_1^2(y)$

$B_1 = T^{-1} \int_0^T du P_1^2(u)$  is a random variable that is the finite time average of the square of the ith power envelope.

A similar procedure is employed for the first term of (A-5); utilizing that result and (A-8) gives

$$\text{Var } (Z|\underline{P}) = T^{-1} (2W_C^{-1} B_C + \sum_{i=S}^n c_i^2 W_1^{-1} B_1) \quad (\text{A-9})$$

$$\text{where } W_C^{-1} = 2 \int_{-\infty}^{\infty} dy \rho_S(y) \rho_0(y)$$

$$B_C = T^{-1} \int_0^T du P_S(u) P_0(u)$$

With regard to the mean value, the condition on the power envelope process is reduced to the condition on a set of random variables  $\{A_i\}$ ,  $i = S, 0, 1, 2, \dots, n$ ; and with regard to the variance, the set of random variables is  $\{B_j\}$ ,  $j = C, S, 0, 1, 2, 3, \dots, n$ . The combined set is a random vector

$$\underline{C} = \{\{A_i\}, \{B_j\}\}$$

For the general case, it is seen that the number of random variables can be large; the exact number depends on the number of non-zero weighting coefficients  $c_i$ . Furthermore,  $A_1$  and  $B_1$  are always dependent, as are  $A_S$ ,  $A_0$ ,  $B_C$ ,  $B_S$ , and  $B_0$ . And in some cases, the sets  $\{A_i\}$  and  $\{B_j\}$  could be dependent.

The probability that the test statistic exceeds zero is the expected value of the conditional probability

$$P_E = \int_0^{\infty} \dots \int_0^{\infty} d\underline{c} f_{\underline{C}}(\underline{c}) N \left\{ \frac{E[Z|\underline{c}]}{\sqrt{\text{Var } [Z|\underline{c}]}} \right\} \quad (\text{A-10})$$

where  $f_{\underline{c}}( )$  is the joint probability density function for the component of  $\underline{C}$ , and where  $E[Z|_ ]$ ,  $\text{Var } [Z|_ ]$  are given by (A-4) and (A-9) respectively.



Distribution List  
for  
"Prediction of Passive Sonar Detection  
Performance in Environments with Acoustical Fluctuations"

<u>Name</u>	<u>Number of copies</u>
Defense Documentation Center Cameron Station Alexandria, VA 22314	12
Office of Naval Research Code 431	2
Code 222	1
Arlington, VA 22217	
Operations Research, Inc. 1400 Spring Street Silver Spring, MD 20910 Attn: Dr. Moses	1
Naval Warfare Research Center Stanford Research Institute Menlo Park, CA 94025	1
Center for Naval Analyses 1400 Wilson Boulevard Arlington, VA 22209 Library	1
Dr. R. Beatty	1
Naval Academy Annapolis, MD 21402 Library	1
Naval Postgraduate School Monterey, CA 93940 Technical Library	1
Naval Air Development Center Johnsville Warminster, PA 18974	1
Naval Ship Research & Development Center Code 1806 Bethesda, MD 20034	1

<u>Name</u>	<u>Number of copies</u>
Naval Ocean Systems Center	
Code 16	1
Code 6212	1
San Diego, CA 92132	
Newport Laboratory	1
Naval Underwater Systems Center	
Newport, RI 02840	
New London Laboratory	2
Naval Underwater Systems Center	
New London, CT 06320	
Naval Ordnance Laboratory	
Silver Spring, MD 20910	
Technical Library	1
Naval Research Laboratory	
Washington, DC 20390	
Code 8109	2
Code 2627	6
Naval Weapons Laboratory (Code K-30)	1
Dahlgren, VA 22448	
Science Applications, Inc.	1
8400 Westpark Drive	
McLean, VA 22101	
Attn: Dr. Cavanagh	
Summit Research Corporation	1
1 West Deer Park Drive	
Gaithersburgh, MD 20760	
Naval Intelligence Support Center	1
4301 Suitland Road	
Washington, DC 20390	
Naval Electronics Systems Command	
Navy Department	
Washington, DC 20360	
Code 320	1
PME-124	1
Naval Sea Systems Command	
Navy Department	
Washington, DC 20360	
Code 06H2	1
Code 06H1	1